CSIRO PUBLISHING

Invertebrate Systematics, 2021, **35**, 59–89
https://doi.org/10.1071/IS20042

A revised phylogeny of the New Caledonian endemic genus *Troglosiro* (Opiliones : Cyphophthalmi : Troglosironidae) with the description of four new species

Gonzalo Giribet[A,C], *Caitlin M. Baker*[A] *and Prashant P. Sharma*[B]

[A]Museum of Comparative Zoology, Department of Organismic and Evolutionary Biology, Harvard University, 26 Oxford Street, Cambridge, MA 02138, USA.
[B]Department of Integrative Biology, University of Madison—Wisconsin, 352 Birge Hall, 430 Lincoln Drive, Madison, WI 53706, USA.
[C]Corresponding author. Email: ggiribet@g.harvard.edu

Abstract. The Cyphophthalmi genus *Troglosiro* (the only genus of the family Troglosironidae) is endemic to New Caledonia, representing one of the oldest lineages of this emerged part of Zealandia. Its species are short-range endemics, many known from single localities. Here we examined the phylogenetic relationships of Troglosironidae using standard Sanger-sequenced markers (nuclear *18S* rRNA, *28S* rRNA, and mitochondrial *16S* rRNA and cytochrome *c* oxidase subunit I) and a combination of phylogenetic methods, including parsimony under Direct Optimization and maximum likelihood with static homology. We also applied a diversity of species delimitation methods, including distance-based, topology-based and unsupervised machine learning to evaluate previous species designations. Finally, we used a combination of genetic and morphological information to describe four new species – ***T. dogny*** sp. nov., ***T. pin*** sp. nov., ***T. pseudojuberthiei*** sp. nov. and ***T. sharmai*** sp. nov. – and discuss them in the broader context of the phylogeny and biogeographic history of the family. A key to the species of *Troglosiro* is also provided.

urn:lsid:zoobank.org:pub:93541314-8309-468C-BB77-B34C3A81137E

Keywords: biogeography, New Caledonia, short-range endemics, species delimitation, Sternophthalmi, unsupervised machine learning.

Received 21 May 2020, accepted 2 August 2020, published online 5 January 2021

Introduction

Among the oldest lineages of New Caledonian endemics is the Cyphophthalmi family Troglosironidae (Harvey *et al*. 2017; Nattier *et al*. 2017; Giribet and Baker 2019), represented by the sole genus *Troglosiro* Juberthie, 1979, with 13 currently recognised species (Juberthie 1979; Shear 1993; Sharma and Giribet 2005, 2009*b*). The family diverged from its sister clade – comprising the families Neogoveidae and Ogoveidae – in the late Palaeozoic, diversifying around the Late Cretaceous–Eocene (Giribet *et al*. 2012; Oberski *et al*. 2018). Around the time when the last species of Troglosironidae were described (Sharma and Giribet 2009*b*), a phylogenetic hypothesis for the family was proposed using parsimony Direct Optimization (Sharma and Giribet 2009*a*). This phylogeny implied an initial divergence between northern and southern species, and suggested the existence of additional species related to *Troglosiro juberthiei* Shear, 1993 (tentatively named *Troglosiro* cf. *juberthiei*), as well as several putative species represented by single or few individuals (females and juveniles) that lacked sufficient diagnostic characteristics for formal description. When this work was completed, methods for species delimitation using DNA sequence data were in their infancy and thus, given the lack of morphological differentiation between *T. juberthiei* and *T.* cf. *juberthiei*, no taxonomic action was taken despite an abundance of specimens for the putative new species.

A recent collecting trip by the authors to New Caledonia yielded additional troglosironid material (Fig. 1, 2) that fills some geographical gaps left in previous studies and allowed us to re-evaluate the identity of *T.* cf. *juberthiei*, for which a plethora of specimens was available. We therefore use current analytical techniques to re-examine the phylogeny and species boundaries of the New Caledonian Cyphophthalmi, which

Fig. 1. Live habitus of three of the described species in this study. *A*, *B*, *Troglosiro sharmai* sp. nov., with a characteristic olive-green colouration when alive. *C*, *D*, *Troglosiro dogny* sp. nov., with the characteristic dotted pattern on the anterior opisthosomal tergites; *C*, female paratype on left, male holotype on the right; *D*, male holotype. *E*, *F*, *Troglosiro pseudojuberthiei* sp. nov.

prompted us to re-study some of the older collections deposited in the Museum of Comparative Zoology (MCZ). Our results led us to revisit the phylogenetic history of the group and describe four new species using a combination of morphological and molecular characters, bringing the number of described species to 17. We further identify three other species for which additional material must be collected before formal description.

Materials and methods

We revisited the collections of Troglosironidae deposited in the Museum of Comparative Zoology, resulting mostly from multiple expeditions conducted by G. B. Monteith during the 2000s, and from the expeditions of P. P. Sharma and J. Y. Murienne in April 2007 and by C. M. Baker and G. Giribet in November 2018. The shelf life (*sensu* Fontaine *et al*. 2012) for the described species is thus between 2 and 19 years, since the oldest specimens were collected in 2001 and the most recent ones in 2018. Specimens were selected for morphological examination (see sections below) as well as molecular study. We combined the new molecular data with those published by Sharma and Giribet (2009*a*) and with unpublished data from the undergraduate senior thesis of P. P. Sharma (2006). The specimens examined, MCZ accession numbers and GenBank codes can be found in

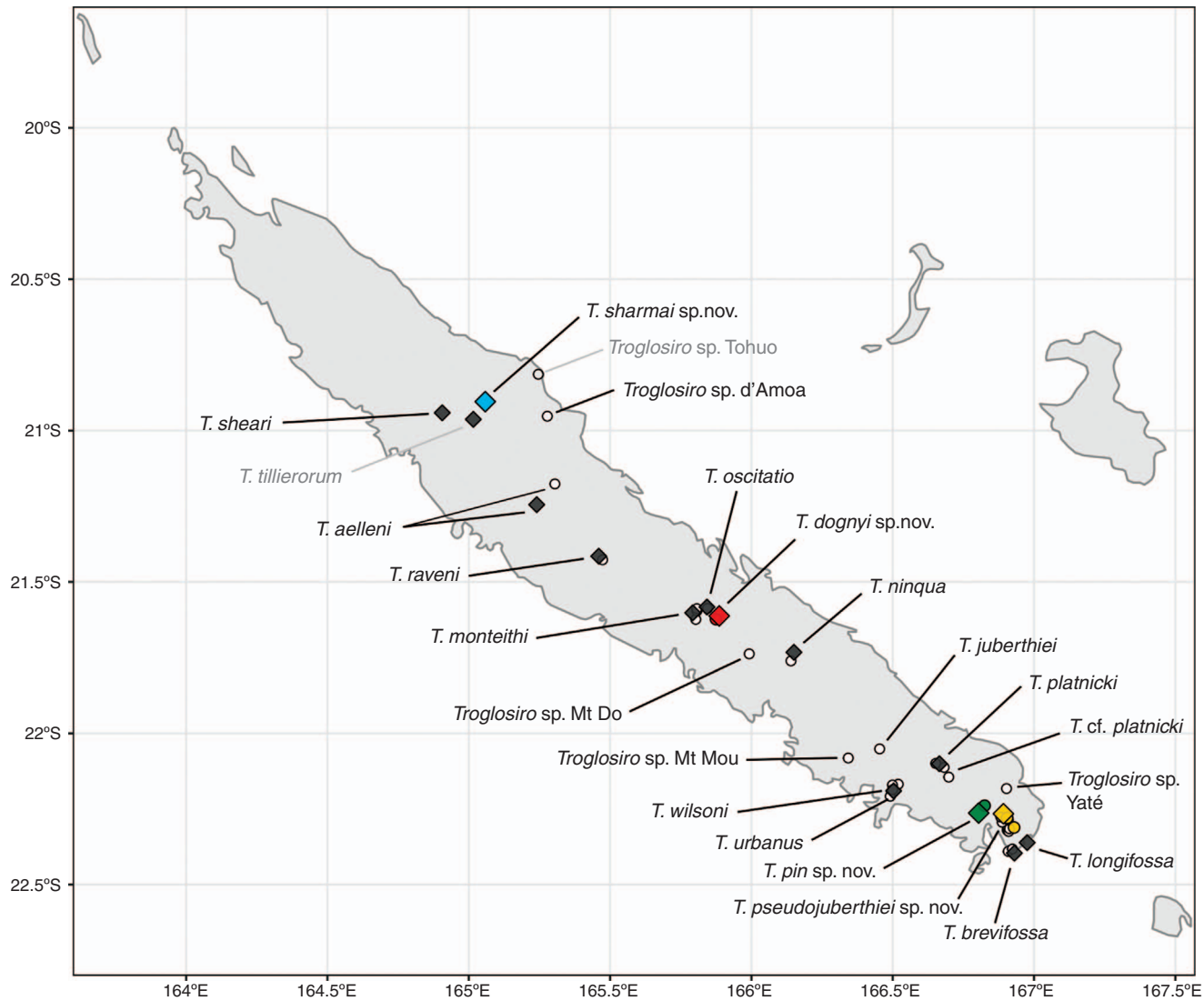

Fig. 2. Distribution map of all known *Troglosiro* localities, most representing specimens used in this study (two names in lighter grey not included). Diamonds represent type localities, grey for the described species and coloured for the four species described from this study. Only *T. juberthiei* lacks a symbol for the type locality, as this was imprecise (Riviere Bleue). Five species (according to sequence data or locality) remain undescribed, as they are represented by non-male singletons.

Table 1. All measurements were taken in Adobe Photoshop CC 2018–20 (Adobe Systems Corporation), using the Image Analysis functions. Measurements of male whole body refer to the holotype; all other measurements refer to the paratype specimens imaged under the scanning electron microscope.

Digital light microscopy images

For each species, the male holotype and one female paratype (when available) were imaged in dorsal, ventral and lateral views using a Keyence VHX 6000 digital microscope (Keyence Corp. Osaka, Japan), which can recognise focus information automatically and create a depth composition image. Because only one male of *T. dogny* sp. nov. is known, we imaged additional characters with the Keyence system, to avoid mounting it for scanning electron microscopy. Because this species is so distinct, based on the external colouration, the lack of SEM details did not prevent us from providing a proper differential diagnosis of the species.

Scanning electron microscopy (SEM)

Specimens prepared for SEM were sonicated for 30 s in a Branson 200 Ultrasonic cleaner and dissected under an Olympus SZX16 stereomicroscope. The appendages, generally of the left side of the specimen, were dissected and mounted in retrolateral view (a few appendages were mounted in prolateral view unintentionally) on a SEM stub using a carbon adhesive tab (Electron Microscopy Sciences, Hatfield, PA, USA). The remaining specimens were mounted on their dorsal side,

Table 1. Specimen information

Taxon IDs and collection accession numbers for all specimens with GenBank accession numbers. Bold indicates new sequences for this study

	MCZ accession number	Locality	Latitude	Longitude	*16S* rRNA	*COI*	*18S* rRNA	*28S* rRNA
OUTGROUPS								
Metasiro savannahensis Clouse & Wheeler, 2014	IZ-134557	Florida, USA	30.56472	–84.95138	DQ825616	DQ825645	DQ825542	DQ825595
Huitaca tama Benavides & Giribet, 2013	IZ-134691	Colombia	7.4	–72.4	DQ518050	DQ518129	DQ518090	DQ825596
Parogovia gabonica (Juberthie, 1969)	IZ-132297	Gabon	0.50448	12.79524	JF935047	JF786411	JF934969	JF935019
Ogovea cameroonensis Giribet & Prieto, 2003	IZ-132315	Cameroon	3.64621	11.29078	JF935026	JF786392	JF934960	JF934994
TROGLOSIRONIDAE		NEW CALEDONIA						
Troglosiro aelleni Shear, 1993	IZ-134764	Aoupinie	–21.18333	165.31666	AY639555	AY639584	AY639497	DQ825580
Troglosiro brevifossa Sharma & Giribet, 2009	IZ-72571	Cap Ndoua	–22.38333	166.91666	–	EU887039	–	EU887117
Troglosiro dogny sp. nov. Juvenile	IZ-51947	Plateau de Dogny	–21.62083	165.87777	–	**MT467216**	–	–
Troglosiro dogny sp. nov.	IZ-151570_2	Plateau de Dogny	–21.61696	165.88393	**MT476270**	**MT467217**	**MT476249**	**MT476257**
Troglosiro dogny sp. nov.	IZ-151570_1	Plateau de Dogny	–21.61696	165.88393	**MT476271**	**MT467218**	**MT476250**	**MT476258**
Troglosiro juberthiei Shear, 1993	IZ-134763_1	Mount Dzumac Road	–22.05	166.46666	EU887077	EU887047	DQ825540	EU887121
Troglosiro juberthiei Shear, 1993	IZ-134763_2	Mount Dzumac Road	–22.05	166.46666	EU887076	EU887048	EU887108	EU887122
Troglosiro juberthiei Shear, 1993	IZ-134767_1	Mount Dzumac Road	–22.05	166.46666	EU887078	EU887049	EU887109	EU887126
Troglosiro juberthiei Shear, 1993	IZ-134767_2	Mount Dzumac Road	–22.05	166.46666	EU887079	EU887050	–	–
Troglosiro juberthiei Shear, 1993	IZ-134767_3	Mount Dzumac Road	–22.05	166.46666	–	EU887051	–	–
Troglosiro juberthiei Shear, 1993	IZ-134767_4	Mount Dzumac Road	–22.05	166.46666	–	EU887052	–	–
Troglosiro juberthiei Shear, 1993	IZ-134767_5	Mount Dzumac Road	–22.05	166.46666	EU887080	EU887060	–	–
Troglosiro longifossa Sharma & Giribet, 2005	IZ-65204_1	Port Boisé Bay	–22.34972	166.97083	DQ518084	DQ518127	DQ518089	DQ825582
Troglosiro longifossa Sharma & Giribet, 2005	IZ-65204_2				–	**MT467219**	–	–
Troglosiro monteithi Sharma & Giribet, 2009	IZ-51948	Col d'Amieu	–21.5925	165.80527	EU887074	EU887043	EU887101	EU887116
Troglosiro ninqua Shear, 1993	IZ-134768	Mount Ningua	–21.75	166.15	DQ518085	DQ518128	DQ518088	DQ825581
Troglosiro oscitatio Sharma & Giribet, 2009	IZ-72572_1	Mount Rembai	–21.58083	165.84333	–	EU887041	EU887106	EU887124
Troglosiro oscitatio Sharma & Giribet, 2009	IZ-72572_2	Mount Rembai	–21.58083	165.84333	–	**MT467220**	–	**MT476259**
Troglosiro pin sp. nov.	IZ-133854_1	Pic du Pin	–22.24713	166.82791	EU887087	EU887062	EU887111	EU887127
Troglosiro pin sp. nov.	IZ-133854_2	Pic du Pin	–22.24713	166.82791	EU887088	EU887063	–	–
Troglosiro pin sp. nov.	IZ-133874_1	Pic du Pin	–22.25	166.81666	EU887085	EU887058	–	–
Troglosiro pin sp. nov.	IZ-133874_2	Pic du Pin	–22.25	166.81666	EU887086	EU887059	–	–
Troglosiro pin sp. nov.	IZ-133875_1	Pic du Pin	–22.25	166.81666	EU887082	–	–	–
Troglosiro pin sp. nov.	IZ-133875_2	Pic du Pin	–22.25	166.81666	**MT476272**	EU887055	–	–
Troglosiro pin sp. nov.	IZ-133875_4	Pic du Pin	–22.25	166.81666	EU887083	EU887056	–	–
Troglosiro pin sp. nov.	IZ-133875_5	Pic du Pin	–22.25	166.81666	**MT476273**	–	–	–
Troglosiro pin sp. nov.	IZ-133876	Pic du Pin	–22.25	166.81666	EU887084	EU887057	–	–
Troglosiro pseudojuberthiei sp. nov.	IZ-151618_1	Pic Du Grand Kaori/ Grand Lac	–22.27977	166.89454	**MT476274**	**MT467221**	**MT476251**	**MT476260**
Troglosiro pseudojuberthiei sp. nov.	IZ-151618_2	Pic Du Grand Kaori/ Grand Lac	–22.27977	166.89454	**MT476275**	**MT467222**	**MT476252**	**MT476261**
Troglosiro pseudojuberthiei sp. nov.	IZ-133855_1	Pic du Grand Kaori	–22.27961	166.89455	EU887089	EU887064	EU887112	EU887128
Troglosiro pseudojuberthiei sp. nov.	IZ-133855_2	Pic du Grand Kaori	–22.27961	166.89455	EU887090	EU887065	–	–
Troglosiro pseudojuberthiei sp. nov.	IZ-133855_3	Pic du Grand Kaori	–22.27961	166.89455	EU887091	EU887066	–	–
Troglosiro pseudojuberthiei sp. nov.	IZ-133856	Pic du Grand Kaori	–22.27961	166.89455	EU887092	EU887067	EU887113	EU887129

(*continued next page*)

Table 1. (*continued*)

	MCZ accession number	Locality	Latitude	Longitude	*16S* rRNA	*COI*	*18S* rRNA	*28S* rRNA
Troglosiro pseudojuberthiei sp. nov.	IZ-133859_1	Pic du Grand Kaori	–22.28333	166.90000	**MT476276**	–	–	**MT476262**
Troglosiro pseudojuberthiei sp. nov.	IZ-133859_2	Pic du Grand Kaori	–22.28333	166.90000	**MT476277**	–	**MT476253**	**MT476263**
Troglosiro pseudojuberthiei sp. nov.	IZ-133859_3	Pic du Grand Kaori	–22.28333	166.90000	**MT476278**	–	–	–
Troglosiro pseudojuberthiei sp. nov.	IZ-133859_4	Pic du Grand Kaori	–22.28333	166.90000	**MT476279**	–	–	–
Troglosiro pseudojuberthiei sp. nov.	IZ-133859_7	Pic du Grand Kaori	–22.28333	166.90000	**MT476280**	–	–	–
Troglosiro pseudojuberthiei sp. nov.	IZ-133859_9	Pic du Grand Kaori	–22.28333	166.90000	**MT476281**	–	–	–
Troglosiro pseudojuberthiei sp. nov.	IZ-133859_10	Pic du Grand Kaori	–22.28333	166.90000	**MT476282**	–	–	–
Troglosiro pseudojuberthiei sp. nov.	IZ-133857_1	Foret Nord	–22.32291	166.91505	EU887093	–	–	–
Troglosiro pseudojuberthiei sp. nov.	IZ-133857_2	Foret Nord	–22.32291	166.91505	EU887094	EU887068	EU887114	EU887130
Troglosiro pseudojuberthiei sp. nov.	IZ-133857_3	Foret Nord	–22.32291	166.91505	EU887095	EU887069	–	–
Troglosiro pseudojuberthiei sp. nov.	IZ-133857_4	Foret Nord	–22.32291	166.91505	EU887096	EU887070	–	–
Troglosiro pseudojuberthiei sp. nov.	IZ-133857_5	Foret Nord	–22.32291	166.91505	EU887097	EU887071	–	–
Troglosiro pseudojuberthiei sp. nov.	IZ-133857_6	Foret Nord	–22.32291	166.91505	EU887098	EU887072	–	–
Troglosiro pseudojuberthiei sp. nov.	IZ-133863_7	Pic du Grand Kaori	–22.28333	166.88333	**MT476283**	–	–	–
Troglosiro pseudojuberthiei sp. nov.	IZ-133863_8	Pic du Grand Kaori	–22.28333	166.88333	**MT476284**	–	–	–
Troglosiro pseudojuberthiei sp. nov.	IZ-133864_4	Pic du Grand Kaori	–22.28333	166.89611	**MT476285**	–	–	–
Troglosiro pseudojuberthiei sp. nov.	IZ-133864_6	Pic du Grand Kaori	–22.28333	166.89611	**MT476286**	–	–	–
Troglosiro pseudojuberthiei sp. nov.	IZ-133864_7	Pic du Grand Kaori	–22.28333	166.89611	**MT476287**	–	–	–
Troglosiro pseudojuberthiei sp. nov.	IZ-133864_8	Pic du Grand Kaori	–22.28333	166.89611	**MT476288**	–	–	–
Troglosiro pseudojuberthiei sp. nov.	IZ-133868_3	Foret Nord	–22.32305	166.91527	**MT476289**	–	–	–
Troglosiro pseudojuberthiei sp. nov.	IZ-133868_4	Foret Nord	–22.32305	166.91527	**MT476290**	–	–	–
Troglosiro pseudojuberthiei sp. nov.	IZ-133868_8	Foret Nord	–22.32305	166.91527	**MT476291**	EU887053	–	–
Troglosiro pseudojuberthiei sp. nov.	IZ-133869	Foret Nord	–22.32305	166.91527	**MT476292**	–	–	–
Troglosiro pseudojuberthiei sp. nov.	IZ-133870_1	Foret Nord	–22.32305	166.91527	**MT476293**	EU887054	EU887104	–
Troglosiro pseudojuberthiei sp. nov.	IZ-133870_4	Foret Nord	–22.32305	166.91527	**MT476294**	–	–	–
Troglosiro pseudojuberthiei sp. nov.	IZ-133870_5	Foret Nord	–22.32305	166.91527	**MT476295**	**MT467223**	–	–
Troglosiro pseudojuberthiei sp. nov.	IZ-133871_1	Foret Nord	–22.316666	166.91666	**MT476296**	–	–	–
Troglosiro pseudojuberthiei sp. nov.	IZ-133871_2	Foret Nord	–22.316666	166.91666	**MT476297**	–	–	–
Troglosiro raveni Shear, 1993	IZ-134777	Col des Rousettes	–21.41666	165.46666	–	EU887042	EU887099	EU887120
Troglosiro sharmai sp. nov.	IZ-151558_1	Near Bopope	–20.91674	165.06189	**MT476298**	**MT467224**	**MT476254**	**MT476264**
Troglosiro sharmai sp. nov.	IZ-151558_2	Near Bopope	–20.91674	165.06189	**MT476299**	**MT467225**	**MT476255**	**MT476265**
Troglosiro sheari Sharma & Giribet, 2009	IZ-134772	Ateou	–20.95	164.91472	–	EU887037	–	–
Troglosiro sheari Sharma & Giribet, 2009	IZ-72565	Ateou	–20.95	164.91472	–	EU887038	EU887100	EU887115
Troglosiro urbanus Sharma & Giribet, 2009	IZ-72577_1	Yahoué	–22.19583	166.49861	EU887073	EU887044	EU887105	EU887118
Troglosiro urbanus Sharma & Giribet, 2009	IZ-72577_2	Yahoué	–22.19583	166.49861	–	EU887040	EU887102	EU887119
Troglosiro wilsoni Sharma & Giribet, 2009	IZ-134787	Mount Koghis	–22.17697	166.51063	EU887075	EU887061	EU887107	EU887125
Troglosiro cf. *platnicki*	IZ-134766	Riviere Bleue	–22.1	166.66666	EU887081	EU887046	EU887110	EU887123
Troglosiro cf. *platnicki*	IZ-134786	Foret Electrique	–22.15	166.68333	–	**MT467226**	–	–
Troglosiro sp. Female	IZ-134781	Pic d'Amoa	–20.95366	165.28783	–	**MT467227**	–	**MT476266**
Troglosiro sp. Juvenile	IZ-134782	Mount Do	–21.7525	166.00083	–	**-**	**MT476256**	**MT476267**
Troglosiro sp. Female	IZ-134783	Mount Mou	–22.06666	166.35000	–	**-**	–	**MT476268**
Troglosiro sp. Female	IZ-134784	Col de Yaté	–22.16805	166.89666	–	**-**	–	**MT476269**

exposing the venter. The specimens were then coated with 10 nm Pt–Pd (80 : 20) in a HAR 050 EMS 300T D dual head sputter coater at the Center for Nanoscale Systems, Harvard University. Specimens were then imaged using an Ultra or Supra FESEM using an SE2 detector with an EHT target of 10 kV. Images were then processed and edited in Adobe Photoshop.

The images of *T. sharmai* sp. nov. were taken first, and unfortunately the biadhesive carbon tape was defective and the scanning electron microscope we used had an alignment problem. These images did not allow for removing backgrounds and have slightly less quality than those of *T. pin* sp. nov. and *T. pseudojuberthiei* sp. nov., which were taken a month later with a different microscope.

Confocal Laser Microscopy (cLSM)

Spermatopositor morphology of three troglosironid species was visualised in 3-D by means of confocal laser scanning microscopy. The spermatopositor was dissected out from the ventral side of the opisthosoma and placed in a Petri dish with alcohol to remove extra tissue carefully with dissecting forceps. Then, the spermatopositor was mounted on a microscope slide with Rapiclear (SunJin Laboratory Co., Hsinchu City, Taiwan) to clear the tissue and covered with a coverslip. We used a Zeiss LSM 880 upright (Carl Zeiss, Jena, Germany) system with an Axio Examiner.Z1 from the Harvard Center for Biological Imaging. Microscope magnifications of 10× and 25× (oil immersion) Plan Apochromat long working distance objectives were used. Laser wavelengths of 405 and 561 nm were used to detect the autoflorescence of the chitin. A series of images (50–65) was taken in the z direction. Maximum intensity or surface 3-D projections were generated and edited with Zen 2 blue edition modular image-processing software (Carl Zeiss, Jena, Germany). All videos are publicly available in MCZbase (http://mczbase.mcz.harvard.edu) in association with specimens' MCZ numbers.

Molecular data

Novel molecular data were generated for four markers (the nuclear rRNA genes *18S* rRNA and *28S* rRNA, and the mitochondrial genes *16S* rRNA and cytochrome *c* oxidase subunit I, *COI*) and combined with existing data for Troglosironidae and outgroups (Sharma and Giribet 2009*a*; Giribet *et al*. 2012). For detailed DNA isolation, amplification and sequencing protocols see these earlier papers, but for most recent specimens, a single leg was used for DNA extraction. In total, we combined data from 77 troglosironid specimens plus 4 outgroup members (3 Neogoveidae and 1 Ogoveidae), which together with Troglosironidae constitute the universally supported clade Sternophthalmi (Giribet and Boyer 2002; Giribet *et al*. 2012). Because the nuclear rRNA genes show no variation within Cyphophthalmi species, not all specimens were sequenced for these markers. Our dataset thus includes 33 *18S* rRNA sequences, 36 *28S* rRNA sequences, 54 *COI* sequences and 65 *16S* rRNA sequences, the last of these being the marker that amplified best for Troglosironidae (Table 1). With these, we constructed different matrices, one containing all markers for all terminals (*M1*), one containing only those terminals with at least two markers (*M2*), and, finally, one containing all those terminals with at least three markers (*M3*). All new sequences have been deposited in GenBank, under accession numbers MT467216–MT467227, and MT476249–MT476299.

Phylogenetic analyses

The different datasets were subjected to a series of phylogenetic analyses, including static (i.e. multiple sequence alignments) and dynamic homology schemes (Wheeler 2003; Wheeler *et al*. 2005), and multiple optimality criteria, including parsimony and maximum likelihood. Analyses were conducted for the individual datasets as well as for a combined dataset using all terminals (81 terminals; matrix *M1*). Additional analyses were conducted for subsets of the data: one for all terminals with two or more loci (51 terminals; *M2*) and one with all terminals with three or more loci (31 terminals; *M3*).

For dynamic homology under parsimony – the chosen method in the study of Sharma and Giribet (2009*a*) – we partitioned the nuclear ribosomal genes into multiple fragments for accommodating missing amplicons in a few of the sequences, as suggested by Wheeler *et al*. (2005). The analyses were based on a Direct Optimization (DO) approach (Wheeler 1996) using POY (ver. 5.1.1, see https://www.amnh.org/research/computational-sciences/poy; Wheeler *et al*. 2015) on a MacBook Pro 2.2 GHz Intel Core i7, 16 GB 1600 MHz DDR3. Initial tree searches were performed using the timed search function in POY, i.e. multiple cycles of (1) building Wagner trees, (2) subtree pruning and regrafting, (3) tree bisection and reconnection, (4) ratcheting (Nixon 1999), and (5) tree-fusing (Goloboff 1999, 2002) [command: search (max_time:00: 01: 00, min_time:00: 00: 10, hits:20, memory: gb:2)] for the combined analysis of all data (matrix *M1*) under equal weights and under a weight scheme *3221*. These two initial trees were used as input for the subsequent analyses. From here, we proceeded to use sensitivity analysis tree fusing (SATF) (Giribet 2007) for a set of six indel or nucleotide change parameters, including linear and non-linear indel extension costs, as in previous studies (e.g. Giribet *et al*. 2014). We conducted three rounds of SATF until tree length stabilised for each of the six parameter sets evaluated. The optimal parameter set was then estimated by using the modified $_{W}$ILD metric (Wheeler 1995; Sharma *et al*. 2011) as a proxy for the parameter set that minimises overall incongruence among data partitions (Table 2). Because the datasets included multiple sequences from the same species, some of the DO analyses spent large amounts of time swapping on equal length trees, and thus for the final analyses we reduced the dataset to only those terminals with three or four genes (matrix *M3*). Trees were drawn using the additive value of indels and base transformations as a proxy for branch lengths [command: trees:(total, branches:true)].

For the static alignment analyses, we generated multiple sequence alignments in MAFFT (ver. 7.4, see https://mafft.cbrc.jp/alignment/software/; Kuraku *et al*. 2013; Katoh *et al*.

Table 2. Direct Optimization analyses

SATF1–3, the number of weighted steps in three rounds of SATF for the six parameter sets evaluated; M2, the weighted steps for matrix M2; *18S*, *28S*, *COI*, *16S* and Total, the weighted steps for the individual partitions for the six parameter sets evaluated; $_{W}$ILD, the associated $_{W}$ILD value

Parameter sets	SATF1	SATF2	SATF3	M2	Individual partitions					$_{W}$ILD
					18S	*28S*	*COI*	*16S*	Total	
111	2398	2398	2398	2278	65	403	1296	598	2398	0.01501
211	2588	2587	2587	2465	66	458	1325	692	2587	0.01778
121	3693	3693	3693	3527	92	580	1948	1009	3693	0.01733
3211	3721	3721	3721	3548	93	579	1960	1019	3721	0.01881
3221	4865	4865	4865	4622	131	816	2626	1212	4865	0.01644
221	4045	4043	4043	3876	94	691	1990	1187	4043	0.02003

2019), using MAFFT-L-INS-i. No post-alignment trimming was conducted, as sequence length variation is minimal for Troglosironidae. However, because genetic distance to the nearest outgroups is very large for some of the mitochondrial genes, we also conducted an analysis excluding mitochondrial genes in the outgroup taxa (matrix *M4*). Removing divergent sequences, even from close outgroups, helps ameliorate issues with short internodes and can increase resolution within the ingroup (Giribet *et al*. 2018). All datasets were analysed using the web version of IQ-TREE (ver. 1.6.11, see http://www.iqtree.org/; Nguyen *et al*. 2015; Trifinopoulos *et al*. 2016), with the substitution model directly estimated by the program, using the Bayesian information criterion as implemented in ModelFinder (Kalyaanamoorthy *et al*. 2017). When combining multiple partitions, an edge-unlinked partition file was selected. Nodal support was estimated using an ultrafast bootstrap analysis with 1000 pseudoreplicates [command: -m MFP -spp -bb 1000].

Input files, alignment files and tree files have been uploaded to the Harvard Dataverse (https://doi.org/10.7910/DVN/ALKFAD).

Species delimitation analyses

Species delimitation is a rapidly growing field and has become a common tool to quantify biodiversity, and many methods are proposed constantly. Here, we used some of the methods designed to deal with simple datasets resulting from single-locus or a few loci obtained under Sanger sequencing, which differ from the family of methods able to detect gene flow, typically applied to genomic datasets. We have chosen methods based on Poisson Tree Processes (PTP) (Zhang *et al*. 2013), a phylogeny-aware method using both the single-rate and the multi-rate PTP (Kapli *et al*. 2017) that incorporates different levels of intraspecific genetic diversity derived from differences in either the evolutionary history or sampling of each species and that does not require an ultrametric tree or defining a sequence similarity threshold. We also examine a distance-based method, Automatic Barcode Gap Discovery (ABGD) (Puillandre *et al*. 2012) that uses sequence alignment data to propose species hypotheses.

PTP and mPTP were run on a server (see https://mptp.h-its.org/#/tree) and allowed for the exclusion of outgroups from the input trees. As input we used three trees, the maximum likelihood tree for all data (matrix *M1*), and the individual maximum likelihood trees for *16S* rRNA and *COI*. For ABGD we ran our analyses on a web server (https://bioinfo.mnhn.fr/abi/public/abgd/abgdweb.html) using the alignments of *16S* rRNA or *COI* with the outgroups removed, with a Kimura80 distance (Kimura 1980).

An unsupervised machine learning approach to delimit species was also employed. This approach, a variational autoencoder (VAE), has previously been shown to accurately delimit closely related species of harvestmen with high population substructure (Derkarabetian *et al*. 2019). In this method, recoded nucleotide data are passed through a neural network (the 'encoder'), which compresses the dimensionality of those data into a reduced representation, wherein each sample has a mean (μ) and standard deviation (σ). This representation is then run through another neural net (the 'decoder'), which generates a reconstruction of the nucleotide data in the form of a two-dimensional plot, where non-overlap of σ is consistent with different species.

VAE was implemented using the Keras python deep learning library (F. Chollet, see https://keras.io) and the TensorFlow machine learning framework (Abadi *et al*. 2016), utilising a python script from Derkarabetian *et al*. (2019) to construct the VAE model and plot the results. DNA alignment data were translated to 'one-hot' encoding such that each nucleotide was given a unique binary variable: A was coded as 1,0,0,0; C was 0,1,0,0; G was 0,0,1,0; and T was 0,0,0,1. Ambiguities from heterozygous sites were also considered, assigning 0.5 to each possible nucleotide (e.g. Y, which could be C or T, was coded as 0, 0.5, 0, 0.5). Missing data and indels (N or –) were coded as 0,0,0,0 and ignored by the model so as to prevent clustering of specimens solely based on the absence of data.

A summary of the species delimitation analyses, including the VAE interpretation of the two-dimensional plots, is inferred by comparing all these methods, the morphological data, and the resulting phylogenetic trees.

Results and discussion

Phylogenetic relationships of Troglosironidae

The best-fit edge-unlinked partition models for the combined analysis of four genes (matrix *M1*) were TIM2+F+G4 (for *16S* rRNA), TNe+I (*18S* rRNA), TVM+F+I+G4 (*28S* rRNA), and GTR+F+I+G4 (for *COI*). The resulting tree is shown in Fig. 3. A very similar model scheme was found for the dataset with

Fig. 3. Phylogenetic analysis of the combined data of four loci (matrix *M1*) with IQ-TREE (ln*L* = –16766.2564). New species appear in bold. Circles at nodes indicate 100% bootstrap support. All other values are indicated in nodes below species (unlabelled nodes had <50% bootstrap support).

three or more genes (*M3*): TIM2+F+G4 (*16S* rRNA), TNe+I (*18S* rRNA), TVM+F+I (*28S* rRNA), and TIM+F+I+G4 (*COI*). The resulting tree is shown in Fig. 4. Phylogenetic analyses of the genetic data indicated that all species represented by more than one individual were monophyletic. The maximum likelihood analyses of the combined datasets (whether using 31, 51 or 81 terminals) generated compatible trees, the sole exception being the interrelationships between *T. wilsoni*, *T. raveni* and *Troglosiro* sp. IZ-134782 (a juvenile specimen from Mount Do that represents an undescribed species). The overall relationships include a basal grade formed by *T. aelleni*, *T. sheari*, *T. sharmai* sp. nov., *T. dogny* sp. nov., *Troglosiro* sp. IZ-134781 (a female from Pic d'Amoa) – all central (*T. dogny* sp. nov.) and northern species – followed by a clade with the remaining terminals, corresponding mostly to central and southern species. These divide into two main clades, one including a group of mostly central species, with *T. wilsoni*, *T. raveni*, *T. monteithi*, *T. ninqua*, *T. oscitatio* and the juvenile from Mount Do. *Troglosiro wilsoni* is the only species that is not geographically located in the central region, and in some analyses (51 terminals dataset; not shown, see Dataverse) appears as sister group to the central clade. Finally, a southern clade includes *T. longifossa*, *T. urbanus*, *T. brevifossa*, *T. platnicki*, *T. juberthiei*, *T. pin* sp. nov., *T. pseudojuberthiei* sp. nov., as well as *Troglosiro* sp. IZ-134783 (a female from Mount Mou). *Troglosiro pin* sp. nov. and *T. pseudojuberthiei* sp. nov. were referred to as *T.* cf. *juberthiei* by Sharma and Giribet (2009*a*), but here they are recognised as two distinct species, neither of which are sister species to *T. juberthiei*. *Troglosiro juberthiei* is instead recovered as the sister group to a series of individuals from Riviere Bleue that we tentatively identify as *T. platnicki*. *Troglosiro* sp. IZ-134784 (a female from Col de Yaté), represented in our dataset by *28S* rRNA only, nests within *T. pin* sp. nov. in the analysis including all data.

The Direct Optimization SATF analysis required three rounds until all parameter sets stabilised in the same tree length. The results found parameter set *111* (all transformations receiving equal weights) to be the optimal parameter set under the $_{W}$ILD criterion, with a tree length of 2398 steps, retaining 42 trees of that length (see Table 2). The strict consensus of this tree showed several collapsed nodes, mostly related to within-species resolution, but also for some of the species. This tree showed *T. dogny* sp. nov. as sister group to all other species, followed by *T. sharmai* sp. nov., and then a clade of *T. aelleni* + *T. sheari*. The remaining species formed a polytomy of *T. wilsoni*; *Troglosiro* sp. IZ-134781; a clade including *T. monteithi*, *T. ninqua* and *T. oscitatio*; a clade comprising *Troglosiro* sp. IZ-134782, *Troglosiro* sp. IZ-134783, *T. raveni*, *T. longifossa*, and *T. urbanus*; and a final clade including *Troglosiro* sp. Yaté IZ-134784, *T. pin* sp. nov., *T. brevifossa*, *T.* cf. *platnicki*, *T. juberthiei* and *T. pseudojuberthiei* sp. nov. Although this topology differs in some aspects from the maximum likelihood counterparts, it shares the grade of *T. dogny* sp. nov., *T. sharmai* sp. nov., *T. aelleni* and *T. sheari v.* all the other species, as well as a southern clade including *Troglosiro* sp. Yaté IZ-134784, *T. pin* sp. nov., *T. brevifossa*, *T.* cf. *platnicki*, *T. juberthiei* and *T. pseudojuberthiei* sp. nov. One difference with the IQ-TREE analysis is that *T. pin* sp. nov. is monophyletic in most of the most parsimonious trees (MPTs), although in two (out of 42) MPTs, *Troglosiro* sp. Yaté IZ-134784 does nest within *T. pin* sp. nov., as in the maximum likelihood analyses.

The DO analysis of the reduced dataset (matrix *M3*), limited to those taxa with three or four genes, is similar to the full analysis (matrix *M1*), but with more resolution (Fig. 5). Parameter set *111* yielded nine trees of 2278 steps, only differing in the intraspecific relationships within *T. juberthiei* and *T. pseudojuberthiei* sp. nov. Here, *T. dogny* sp. nov. also appears as the sister group to all the other *Troglosiro* species, followed by *T. sharmai* sp. nov., then by the clade composed of *T. aelleni* and *T. sheari*; again, all these taxa form a grade, as in the IQ-TREE analyses. The remaining species are recovered in this analysis in two major clades, one including the southern species *T. pin* sp. nov., *T.* cf. *platnicki*, *T. juberthiei* and *T. pseudojuberthiei* sp. nov., and a second clade including *T. monteithi*, *T. ninqua*, *T. oscitatio*, *T. wilsoni*, *T. raveni*, *T. longifossa* and *T. urbanus*, i.e. a clade including central and southern species.

Determining whether the North species form a grade (as in the maximum likelihood analyses and most parameter sets for DO) or a clade (as in DO under parameter set *3211*; see Fig. 5) is beyond the resolution power of the chosen Sanger markers, as evidenced by the low nodal support in the basal-most nodes of the tree; this effect may also be partly attributable to the long distance to the outgroup. However, nearly all analyses find strong divisions between northern, central, and southern species, with the exception of two high-elevation taxa, *T. dogny* sp. nov. and *T. wilsoni*, which belong to the Northern and Central groups, despite being located in the centre and south, respectively.

Species delimitation

We conducted a species delimitation analysis using PTP and mPTP for the combined dataset (*M1*) as well as for the individual *COI* and *16S* rRNA datasets using only *Troglosiro* sequences. Additionally, we ran ABGD and VAE analyses for the individual *COI* and *16S* rRNA datasets, excluding outgroups. Results varied across analyses, largely as a function of underlying method. These are presented in Fig. 6, where each species estimation is represented by a coloured box (singleton species estimates are shown in white). The VAE σ-clusters are shown in Fig. 7. When comparing methods, mPTP and VAE always estimated fewer species than PTP, whose results were nearly identical to those of ABGD; the latter two methods estimated 12 species for *16S* rRNA and 17 for *COI*. Although these results may at first look different, 5 of the species estimated by the *COI* dataset were not present in the *16S* rRNA dataset, implying no incongruence between PTP and ABGD. On the other hand, mPTP and VAE tended to group species, especially for those represented by one or a few specimens (Fig. 6, 7). Some of these 'large' groups of specimens involved some of the new species described here. For matrix *M1*, *T. pin* sp. nov. and *T. pseudojuberthiei* sp. nov. were estimated to be a single species, but the single locus analyses of mPTP and all other methods treated both as separate species, and all analyses found them to be distinct from *T. juberthiei*, where these

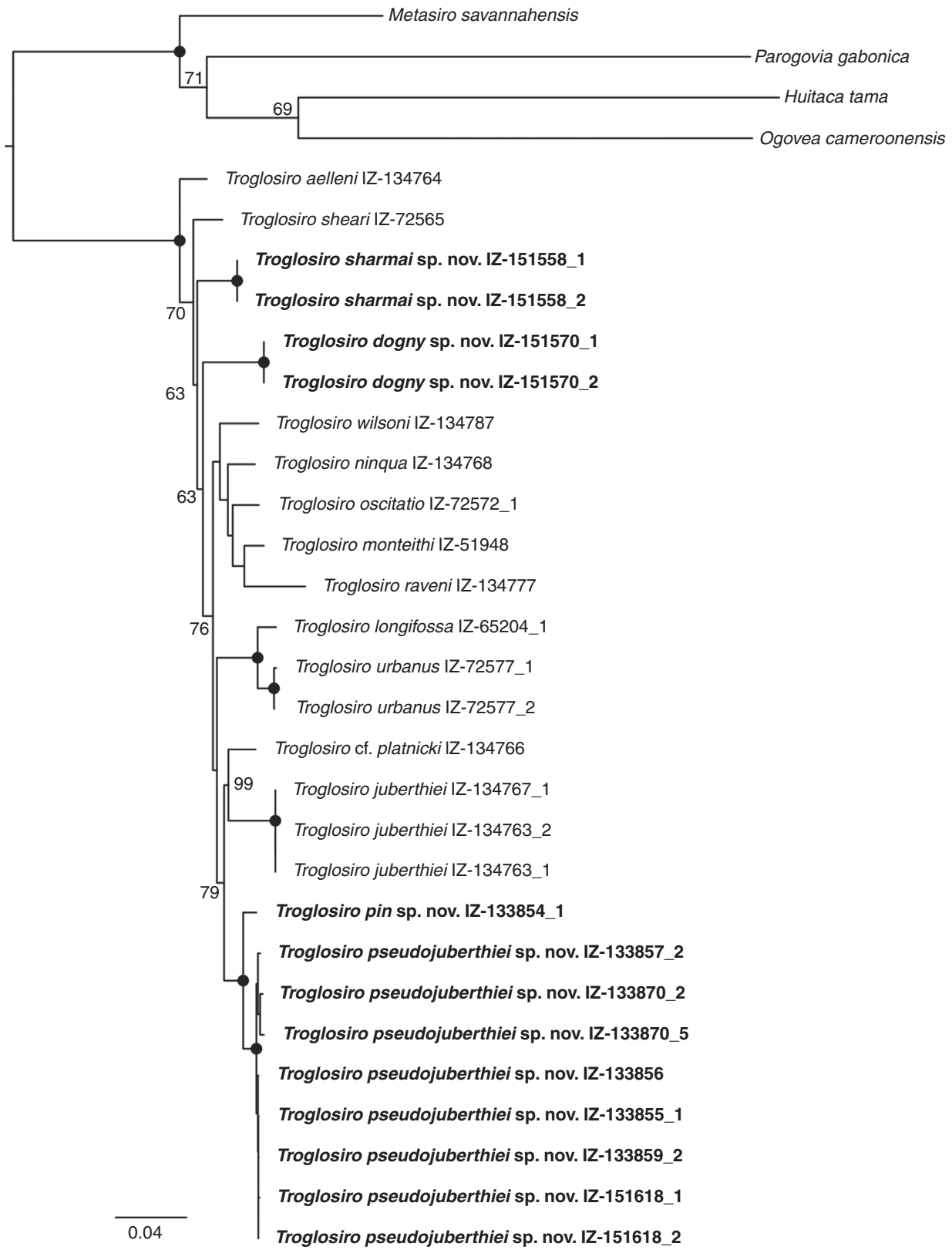

Fig. 4. Phylogenetic analysis of the combined data of taxa with three or more loci (matrix *M3*) with IQ-TREE (ln*L* = –16165.349). New species appear in bold. Circles at nodes indicate 100% bootstrap support. All other values are indicated in nodes below species (unlabelled nodes had <50% bootstrap support).

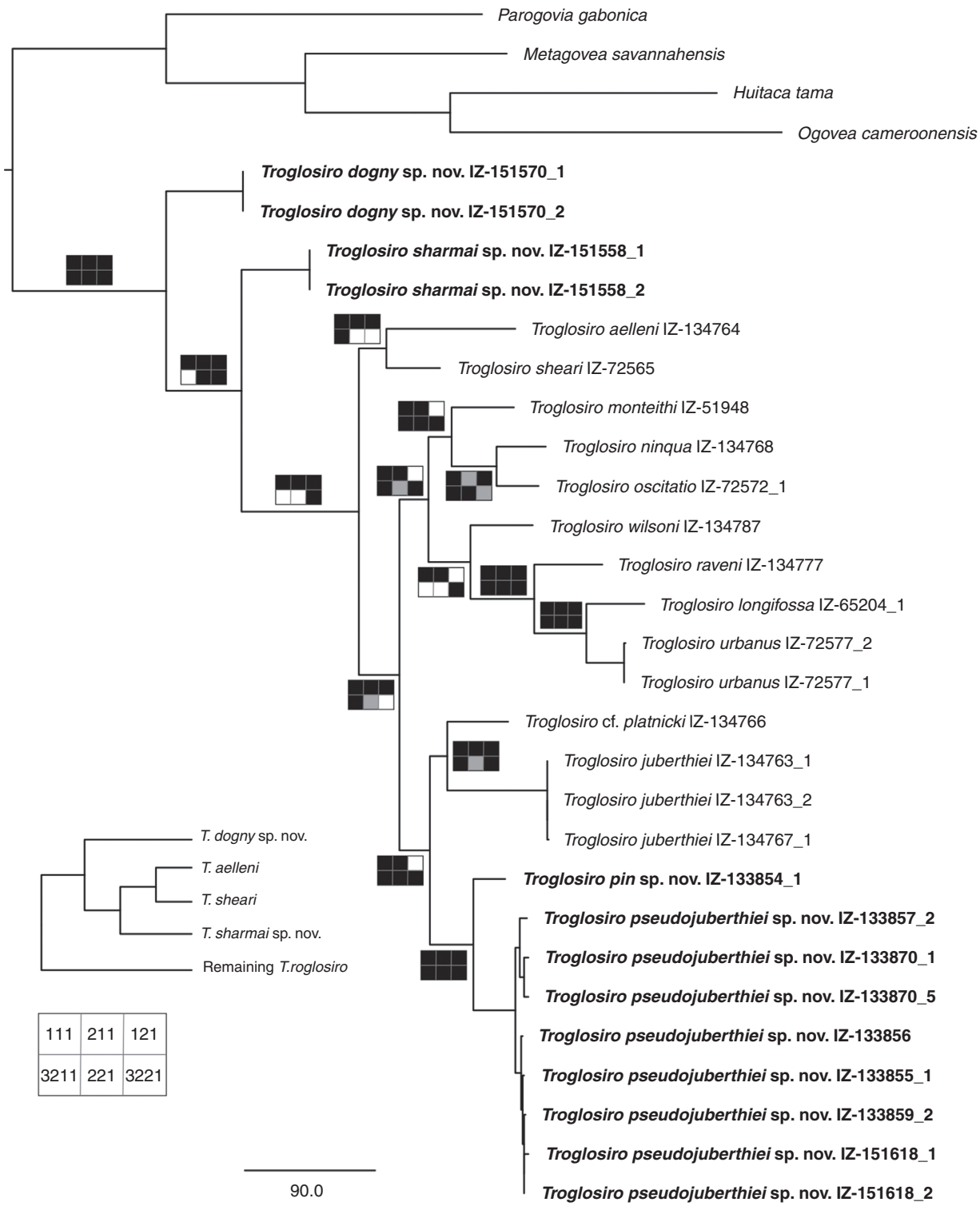

Fig. 5. Phylogenetic analysis of the combined data of taxa with three or more loci (matrix *M3*) under direct optimization. The tree is one of nine equally parsimonious trees for parameter set *111* at 2278 steps (other trees differ only in the internal branching of *T. juberthiei* and of three specimens of *T. pseudojuberthiei* sp. nov. [IZ-133859_2, IZ-151618_1 and IZ-151618_2]). Sensitivity plots on nodes indicate whether that node is found in other parameter sets (see legend), with black indicating monophyly, white as non-monophyly and grey as monophyly under some of the most parsimonious trees. Left inset shows alternative topology under parameter set *3211*, which finds a clade composed of *T. dogny* sp. nov., *T. aelleni*, *T. sheari* and *T. sharmai* sp. nov. as the sister group to all other species.

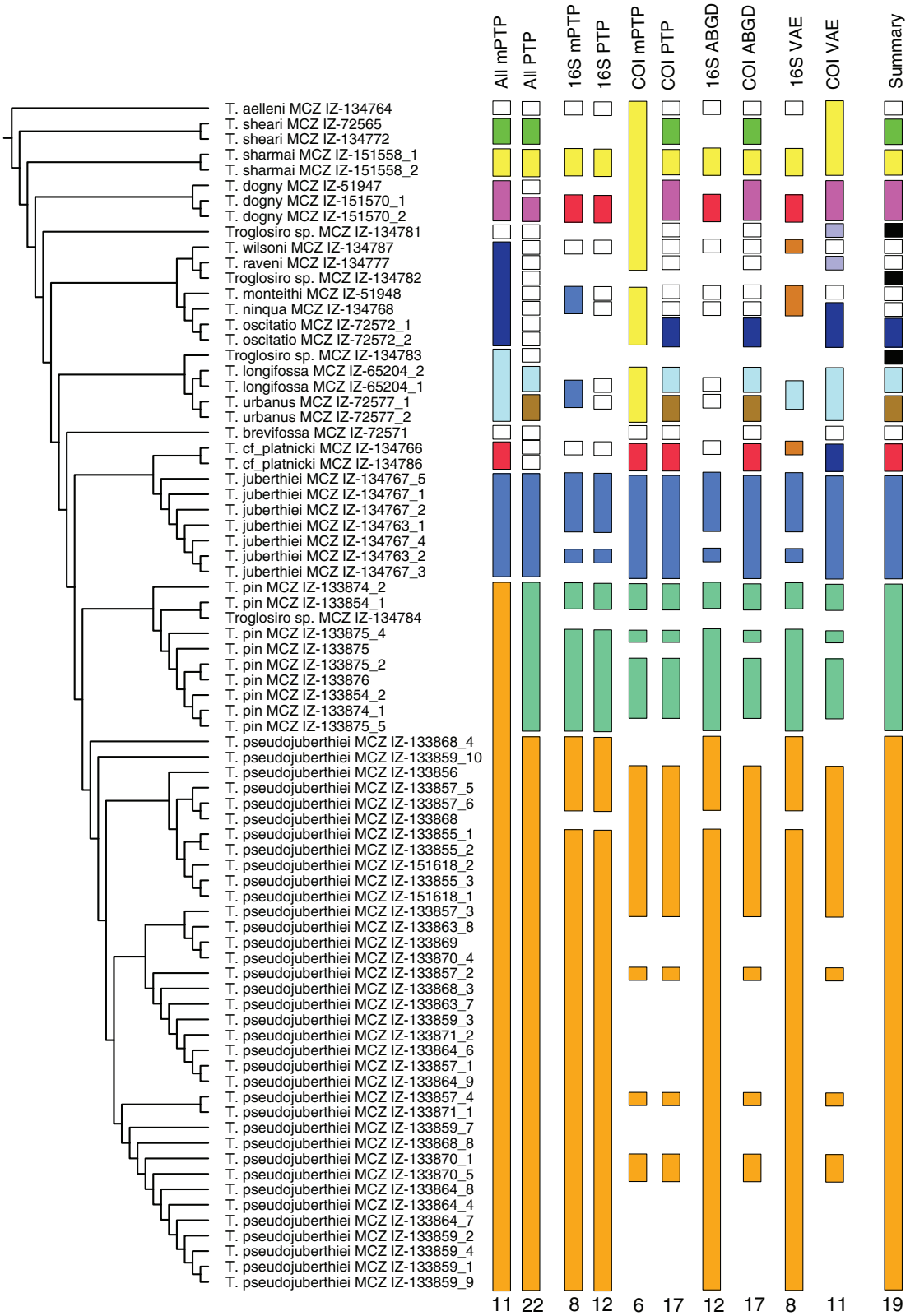

Fig. 6. Species delimitation results mapped on the maximum likelihood tree of matrix *M1* without outgroups. Coloured bars at right show the summary of species delimitation analyses, each colour representing a species, white squares representing singletons of different species and black squares putative species not described in this study. From left to right: mPTP and PTP analyses of the combined dataset, mPTP and PTP analyses of the *16S* rRNA dataset, mPTP and PTP analyses of the *COI* dataset, ABGD analyses of the *16S* rRNA and *COI* datasets, VAE analyses of the *16S* rRNA and *COI* datasets, and summary of species hypotheses combining the species delimitation analyses and phylogenetic results.

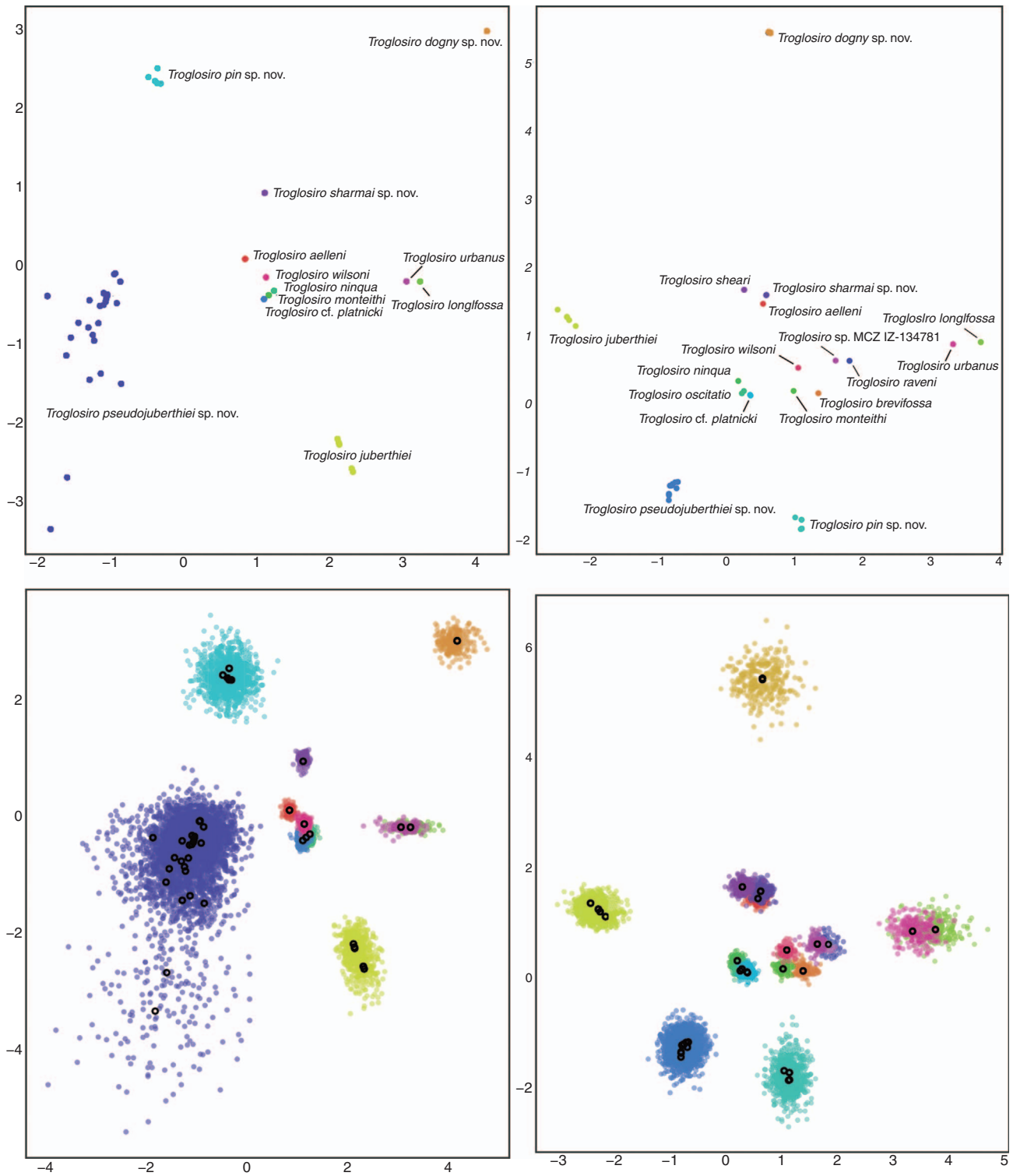

Fig. 7. VAE results. Top: results with encoded mean (μ) and inferred species names for *16S* rRNA (left) and *COI* (right). Bottom: results with encoded mean (μ – open circles) and standard deviation (σ – closed circles) for *16S* rRNA (left) and *COI* (right). Species hypotheses were assigned *a priori*. Based on the criterion of mostly non-overlapping standard deviations, *16S* rRNA suggests eight species, clustering *T. longifossa–T. urbanus* and *T. wilsoni–T.* cf. *platnicki–T. ninqua–T. monteithi*. *COI* grouped the putative species *T. longifossa–T. urbanus*, *T. sheari–T. sharmai* sp. nov.*–T. aelleni*, *T. ninqua–T. oscitatio–T.* cf. *platnicki*, and *T. raveni–Troglosiro* sp.

specimens were tentatively placed by Sharma and Giribet (2009*a*). For the *COI* dataset, mPTP found *T. dogny* sp. nov. and *T. sharmai* sp. nov. to be part of the same putative species – together with most other northern and central species, including *T. aelleni*, *T. longifossa*, *T. monteithi*, *T. ninqua*, *T. oscitatio*, *T. raveni*, *T. sheari*, *T. urbanus*, *T. wilsoni* and *Troglosiro* sp. IZ-134781 – but again, all other analyses identified *T. dogny* sp. nov. and *T. sharmai* sp. nov. as two putative species. The *COI* dataset analysed with VAE also grouped *T. sharmai* sp. nov. with two other species, in this case *T. aelleni* and *T. sheari*, basically grouping the first three splits of the tree. Overall, most analyses (including all PTP and ABGD analyses) resolved each named species as a putative species, whether represented by one or more specimens) and recognised the four species described below, with some analyses identifying three additional species (black squares in Fig. 6) that could not be described due to the lack of adult males for anatomical examination. These three additional species are *Troglosiro* sp. IZ-134781, *Troglosiro* sp. IZ-134782 and *Troglosiro* sp. IZ-134783. All three were collected in 2004 and originally preserved in propylene glycol, followed by 70% EtOH.

Troglosiro sp. IZ-134781 is known from a single female from Pic d'Amoa. This specimen appears as a separate lineage in all analyses, as the sister group to the central and southern species. Pic d'Amoa is quite isolated from other known *Troglosiro* localities and future field work should provide specimens to properly describe this putative species. *Troglosiro* sp. IZ-134782 is likewise known by just one juvenile from Mount Do, which unfortunately did not amplify for the mitochondrial markers. This species appears as the sister group to *T. raveni*, a species found far away, and is most certainly not the same as *Troglosiro* sp. IZ-134782, although until additional sampling effort is conducted it will remain undescribed. Finally, *Troglosiro* sp. IZ-134783 is known from a single female from Mount Mou, a locality relatively close to the type locality of *T. juberthiei*, but it is the sister group to *T. longifossa* + *T. urbanus*. Unfortunately, this species is represented only by *28S* rRNA data.

One more unidentified specimen remains, a specimen from Col de Yaté (MCZ IZ-134784), known from a single female collected in 2005 and sequenced only for *28S* rRNA. The analyses including the *28S* rRNA data place this specimen within *T. pin* sp. nov., from a relatively close locality. For the time being we leave this specimen unassigned, but it is less likely that it constitutes a new species, as mPTP analyses of the *28S* rRNA data were not able to distinguish among species and PTP recognised 22 species, grouping *Troglosiro* sp. IZ-134784 with *T. pin* sp. nov. Further sequencing of fresh specimens around this locality should help understand whether *T. pin* sp. nov. is restricted to the type locality and its surroundings, or if it has a broader geographic range, something rare in *Troglosiro*.

Finally, a female specimen collected by G. Monteith at 400-m elevation in the Touho TV tower (MCZ IZ-134785) (Fig. 2) and not sequenced, almost certainly represents another undescribed species that remains to be collected and formally named.

Systematics and biogeography of Troglosironidae

As concluded in earlier work, troglosironids constitute an extreme case of short-range endemism (*sensu* Harvey 2002), with a probable large amount of undescribed diversity (according to Sharma and Giribet 2009*b*). This latter study suggested the possible lack of differentiation between *T. juberthiei* and *T. platnicki*, both species from Rivière Bleue. Our analysis of *Troglosiro* relationships with expanded taxonomic sampling supports instead the inference that the two species are reciprocally monophyletic sister taxa, and species delimitation analyses consistently supported their validity as separate entities. More generally, species of *Troglosiro* closely accord with the quintessential biogeographic trends exhibited by Cyphophthalmi, with patterns of cladogenesis reflecting high fidelity for the geography of New Caledonia. The subdivision of species groups into northern, central, and southern clusters likely reflects progressive colonisation of Grande Terre in the Eocene–Oligocene.

Key to historical biogeographic study of Troglosironidae is deciphering the origins of this relictual genus. Whereas all other mite harvestmen lineages accord closely with the geological histories of the landmasses they inhabit, Troglosironidae is known only from New Caledonia and its closest sister groups do not occur in other parts of Zealandia or Australia (to which the basement of Grand Terre was once connected). The sister taxon of *Troglosiro* comprises a distant clade of tropical Gondwanan lineages that diverged from their New Caledonian cousins in the Permian or Carboniferous (Giribet *et al*. 2012; Oberski *et al*. 2018), offering no clues as to the biogeographic history of Troglosironidae before the re-emergence of Grand Terre after its ophiolitic obduction in the Eocene (Sutherland *et al*. 2020). Like *Amborella trichopoda* (another New Caledonian endemic) or the leiopelmatid frogs of New Zealand (endemic to New Zealand, sister group to a North American genus), *Troglosiro* remains an obdurate biogeographic mystery. In the absence of a closely related sister group outside of New Caledonia, available data for *Troglosiro* accord neither with the geological history of Grand Terre's former connection to Zealandia, nor with recent dispersal from any known landmass (Sharma and Giribet 2009*a*). Future surveys of Cyphophthalmi must prioritise the sampling of primary forest habitats of tropical Gondwanan and eastern New Guinean terranes that have escaped previous collecting campaigns, towards possibly discovering a living sister lineage of *Troglosiro*. Recent discoveries extending known mite harvestman distributions, stemming from renewed interest in this taxon as a biogeographic model over the past two decades, may serve as promising heralds for a future resolution of troglosironid origins (Clouse and Giribet 2007; Giribet *et al*. 2007; Clouse *et al*. 2011; Giribet 2011; Schmidt *et al*. 2019).

Taxonomic section

Family **TROGLOSIRONIDAE** Shear, 1993
Genus ***Troglosiro*** Juberthie 1979
Troglosiro sharmai Giribet & Baker sp. nov.
(Fig. 1*A*, *B*, 8–11)

urn:lsid:zoobank.org:act:7701F07E-9F0A-43CA-882A-96BD35D824EC

Material examined

Holotype. Male (MNHN, ex. MCZ IZ-151558) from rest area by La Tiwaka river (–20.91674°, 165.06189°, 98-m elevation), near Bopope, Province Nord (New Caledonia), C.M. Baker & G. Giribet, leg., 11.xi.2018, collected by sifting leaf litter.

Paratypes. 6 males (1 leg of two males used for DNA extraction; 1 dissected for spermatopositor study), 11 females (MCZ IZ-151558), same collecting data as holotype.

Additional material. 1 female preserved in RNA*later*, transferred to MCZ cryo-collection, same collecting data as holotype; 1 juvenile preserved in RNA*later* and used to sequence its transcriptome (SRR11812289), same collecting data as holotype.

Diagnosis

Troglosironid with a conspicuous body colouration combining darker and lighter patterns (Fig. 1*A*, *B*, 8) reminiscent of *T. raveni*. The species is similar to other northern species in lacking an opisthosomal depression (Fig. 8*B*, 9*A*, *D*), as also found in *T. aelleni*, *T. juberthiei*, *T. raveni*, *T. sheari* and *T. tillierorum*. It can be distinguished from these other northern species by the sternal opisthosomal pores, as it has two fused pores towards the centre of the midline of sternite 3 and one near the anterior side of the midline of sternite 4 (Fig. 9*D*, 10*A*), followed by two smaller pores on sternites 4 and 5, a condition most similar to *T. raveni*. Furthermore, *T. sharmai* sp. nov. and *T. aelleni* lack a dorsal crest on the basal cheliceral article, but they can be distinguished by their size and colouration pattern, as *T. aelleni* is a lightly pigmented species whereas *T. sharmai* sp. nov. has a distinct colouration pattern. Spermatopositor (Fig. 11*K*, *L*) most similar to that of *T. tillierorum*, but in *T. sharmai* sp. nov. the spermatopositor lacks ventral microtrichiae, the ventral plate is more pointed and the apical microtrichiae are positioned more distally than in *T. tillierorum* (see Shear 1993, fig. 16).

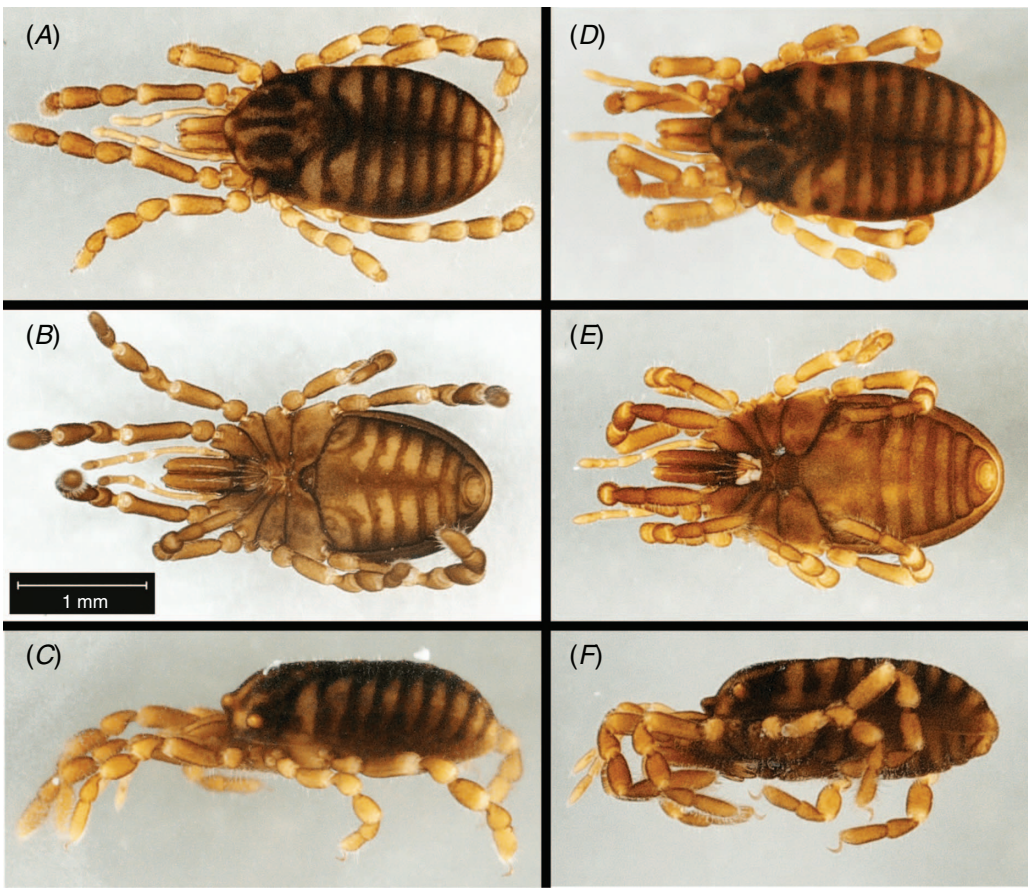

Fig. 8. *Troglosiro sharmai* sp. nov., stereomicroscope views of male holotype (MCZ IZ-151558) (*A–C*) and female paratype (MCZ IZ-151558) (*D–F*). *A*, Dorsal view. *B*, Ventral view. *C*, Lateral view, left side. *D*, Dorsal view. *E*, Ventral view. *F*, Lateral view, left side. Scale bar applies to all images.

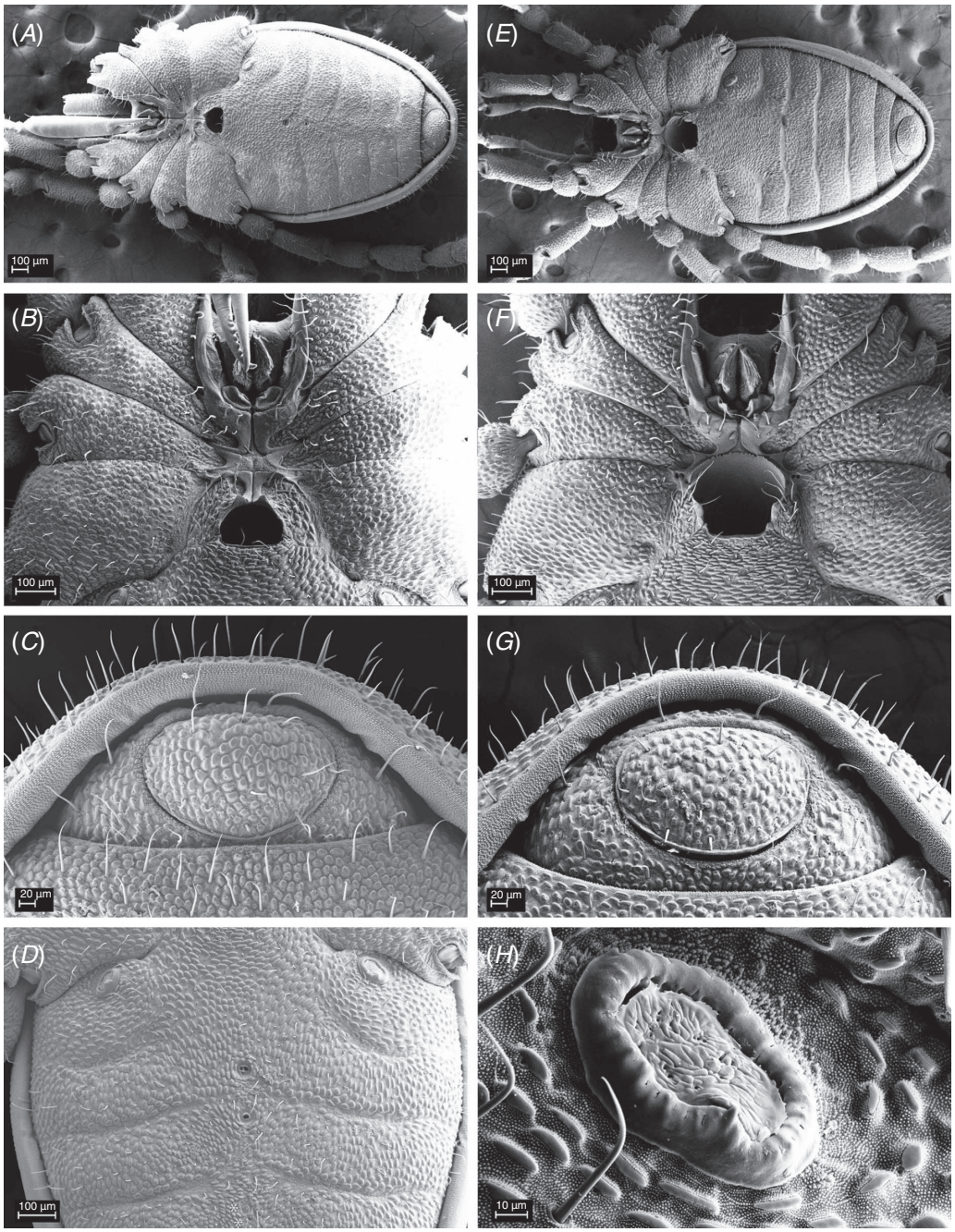

Fig. 9. *Troglosiro sharmai* sp. nov. scanning electron micrographs of paratypes (MCZ IZ-151558). *A*, Male, ventral view. *B*, Male, prosoma, sternal region. *C*, Male, anal region. *D*, Male opisthosomal sternal region with glandular opening pores (posterior pores covered by secretion). *E*, Female, ventral view. *F*, Female, prosoma, sternal region. *G*, Female, anal region. *H*, Male, left spiracle.

Description of male

Total length of male holotype 2.21 mm; width at widest point, at the third opisthosomal segment, 1.19 mm; length : width ratio 1.95; width across ozophore tips 1.07 mm. Body with a banded pattern of dark brown and a tint of olive green in the live specimens, unlike that observed in any other live Cyphophthalmi (Fig. 1*A*, *B*) which appears brown and yellow when fixed in ethanol; legs light brown. Body surface with tuberculate–microgranulate microstructure (*sensu* Murphree 1988) across its entire surface (Fig. 9).

Ozophores conical, of type 2 of Juberthie (1970; see also Giribet 2003). Eyes absent. Transverse opisthosomal sulci conspicuous. Mid-dorsal longitudinal opisthosomal sulcus

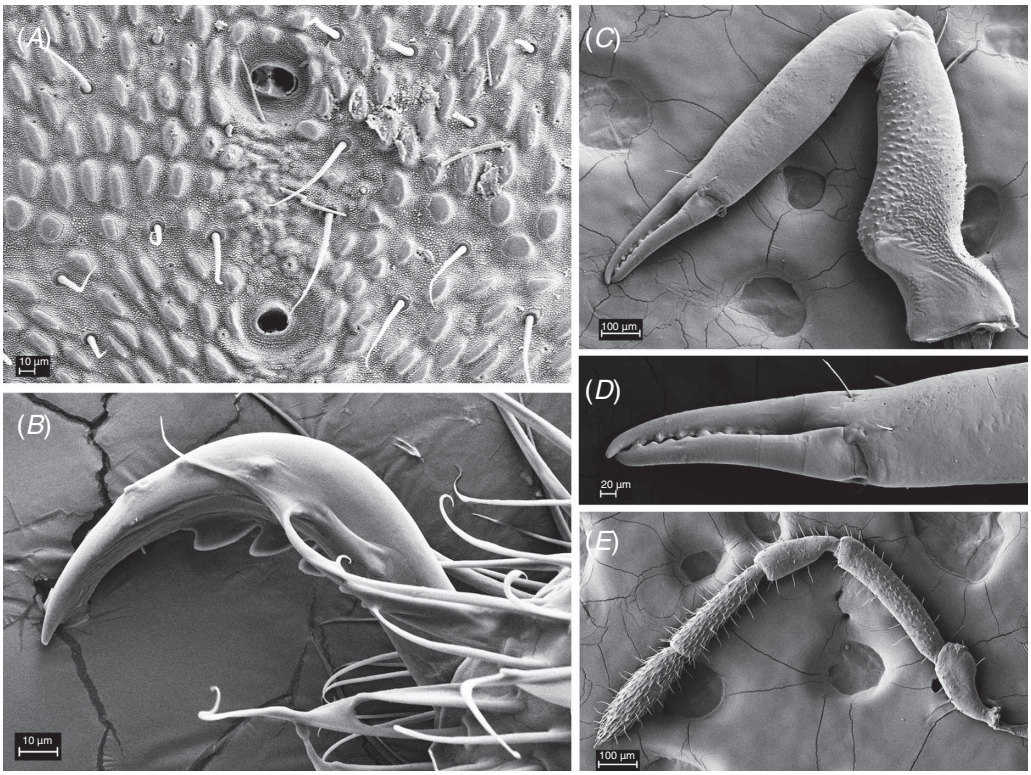

Fig. 10. *Troglosiro sharmai* sp. nov. scanning electron micrographs of paratypes (MCZ IZ-151558). *A*, Male, detail of opisthosomal sternal region (sternites 3 and 4) with glandular opening pores. *B*, Male, left claw II. *C*, Female, right chelicera, retrolateral view. *D*, Female, right chelicera, detail of cheliceral finger. *E*, Male, left palp, retrolateral view.

present. Posterior end of body evenly rounded. Opisthosomal sternites not depressed; with two large and two smaller sternal pore openings along midline of opisthosomal sternites (Fig. 9*A*, *D*). Anteriormost opisthosomal sternal pore double, towards middle of sternite 3; second pore towards anterior end of sternite 4; two smaller pores opening on posterior of tergite 4 and anterior part of sternite 5 (not clearly visible in SEM images, as they may contain secretion, but indicated with an asterisk in Fig. 9*D*).

Coxae of legs I and II movable, coxae of legs III and IV fused. Ventral prosomal complex of male with coxae of legs II, III and IV meeting in the midline, coxae I not so. Sternum absent. Gonostome semicircular, width (167 µm) greater than length (108 µm) (Fig. 9*B*).

Spiracles in the form of a closed circle (Fig. 9*H*), with maximum diameter 94 µm. Sternites 8 and 9 and tergite IX fused, forming a corona analis (Fig. 9*C*). Anal plate without conspicuous modifications, in ventral position (Fig. 9*C*); 246 µm wide, 163 µm long. Anal gland pores absent.

Chelicerae (Fig. 10*C*) without a dorsal crest; with few setae. Granulation restricted to the proximal article. Proximal article 708 µm long, 230 µm deep, with a single posterior ventral process. Second article 880 µm long, 144 µm deep, widest near the first third of its length; dentition with alternation of small and large nodular teeth in the fixed finger (Fig. 10*D*). Distal article 297 µm long, 65 µm deep, dentition regular.

Palp (Fig. 10*E*) without ventral process on proximal end of trochanter; without conspicuous modifications, and sparse ornamentation present on second segment only. Length/width (µm) (length : width ratio in parentheses) of palpal articles from trochanter to tarsus: 224/107 (2.1); 389/78 (4.9); 235/86 (2.7); 315/84 (3.7); 286/96 (2.9); total length 1.45 mm. Palpal claw 45 µm long.

Legs robust (Fig. 11*A–D*); surfaces of all trochanters, femurs, patellae, tibiae and metatarsi thickly and uniformly granulated, except for retrolateral sides of trochanters III and IV, retrolateral area of the distal part of femur III, and the whole retrolateral part of patella and tibia III (Fig. 11*C*). Tarsi not appreciably ornamented (Fig. 11*E–H*). Tarsus I with a distinct solea (Fig. 11*E*). Dorsum of tarsi I (Fig. 11*E*) and II (Fig. 11*F*) with conspicuous solenidia, trichomes and sensilla chaetica (Juberthie 1979; Willemart and Giribet 2010). Tarsal claws I (Fig. 11*E*), III (Fig. 11*G*) and IV (Fig. 11*H*) smooth, tarsal claw II with five teeth tapering in size from distal to proximal (Fig. 10B, 11F). For leg measurements for each article (length/max depth) see Table 3.

Leg formula: I > IV > II > III. Tarsus IV of male not divided, carrying a small lamelliform adenostyle proximal to most basal region of tarsus (Fig. 11*H*). Adenostyle (Fig. 11*J*) 86 µm long, slightly curved, and acutely triangular.

Spermatopositor 420 µm long × 200 µm wide (Fig. 11*K*, *L*); without ventral microtrichia, 3 lateral microtrichiae on

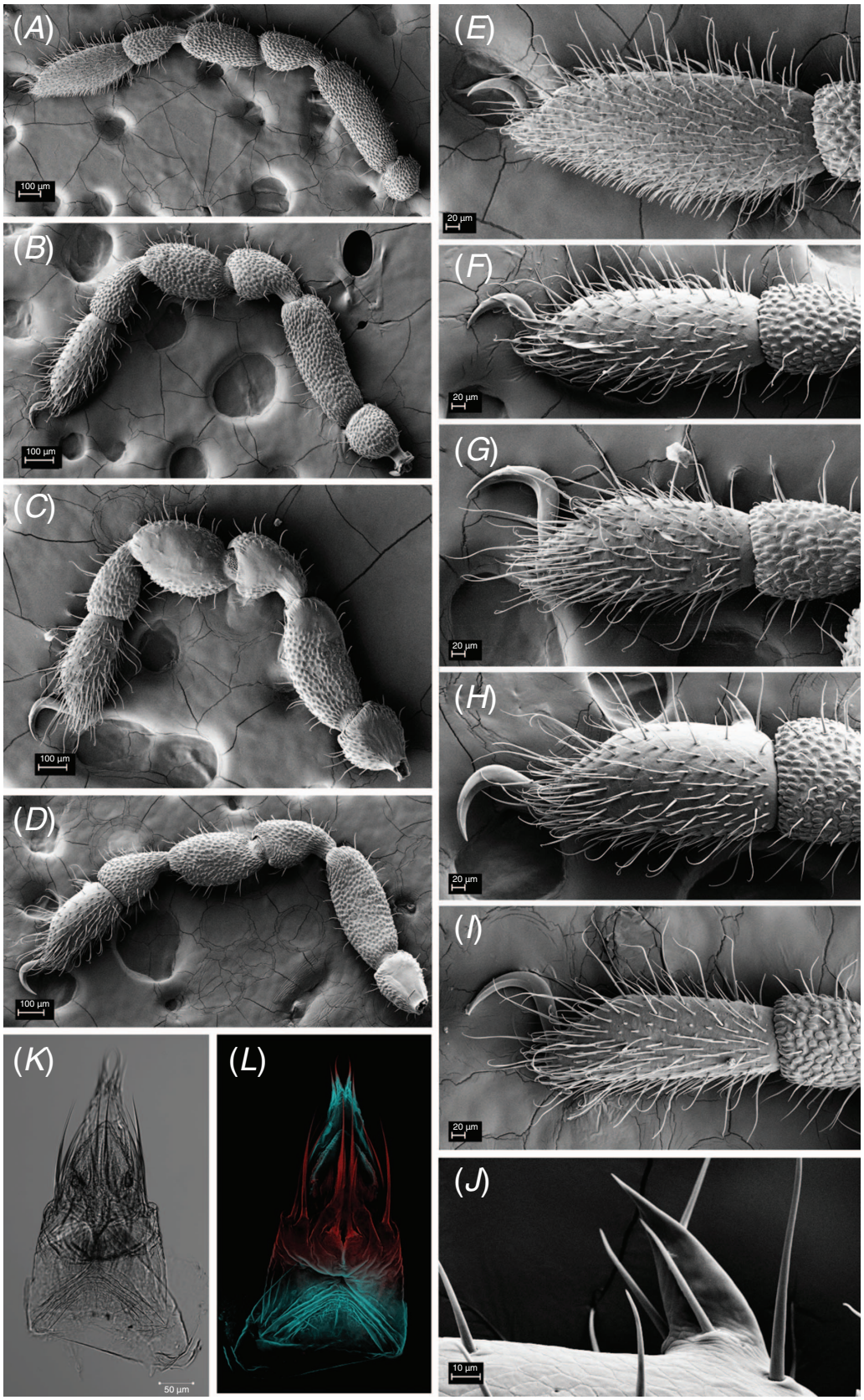
(A)
100 µm
(B)
100 µm
(C)
100 µm
(D)
100 µm
(E)
20 µm
(F)
20 µm
(G)
20 µm
(H)
20 µm
(I)
20 µm
(J)
10 µm
(K)
50 µm
(L)

Table 3. Measurements for each leg article (μm) (length/maximum depth) for *T. sharmai*
Tr, trochanter; Fe, femur; Pa, patella; Ti, tibia; Mt, metatarsus; Ta, tarsus; L, length. All leg measurements are in micrometres (except where specified otherwise)

	Tr	Fe	Pa	Ti	Mt	Ta	Total L (mm)
Leg I	165/200	557/196	325/188	334/183	306/155	457/186	2.144
Leg II	191/174	455/177	295/185	285/190	273/148	353/140	1.852
Leg III	188/188	363/177	261/188	267/206	238/140	299/144	1.616
Leg IV	221/185	475/197	326/200	328/215	294/199	369/189	2.013

each side, and a cluster of 4 dorsal setae, with the centralmost pair about half the length of the immediately adjacent pair. All four dorsal microtrichiae with enlarged bases. Ventral plate enlarged, arrow-shaped, with a rugose edge; movable fingers enlarged, reaching about half of the plate length and serrated lateral margins. Four short apical microtrichiae with scaly bases, narrow, extending well beyond ventral plate.

Description of female

Total length of female paratype (Fig. 8*D–F*) 2.32 mm; width at widest point 1.26 mm; length : width ratio 1.84; width across ozophores 1.12 mm. Ventral prosomal complex (Fig. 9*E*, *F*) with only coxae II meeting in the midline; coxae I, III and IV not meeting in the midline (Fig. 9*F*); gonostome subpentagonal, with a fringed anterior margin (Fig. 9*F*). Opisthosomal sternites without conspicuous modifications and without sternal glandular pores. Anal region without modifications (Fig. 9*G*); anal plate 250 × 160 μm. Tarsus of leg IV smooth, without modification, its dorsal side not flattened (Fig. 11*I*). Ovipositor not studied.

Distribution

Known only from a single locality on the banks of La Tiwaka river.

Remarks

Troglosiro sharmai sp. nov. was collected in a disturbed habitat near a river bank and close to a private property when searching for *T. tillierorum* Shear, 1993, whose type locality is ~10 km distant (type locality is –20.953611, 165.016944, 350-m elevation, but we could not find suitable accessible habitat near these coordinates). Its spermatopositor is most similar to that of *T. tillierorum*, but that of *T. sharmai* sp. nov. is more elongate, especially its ventral side, which extends well beyond the ventral plate. *Troglosiro sharmai* sp. nov. is conspicuously similar to *T. raveni* Shear, 1993 in displaying a specific colouration pattern with bands of lighter colour, but the two species are not related phylogenetically. *Troglosiro tillierorum* does not share this colouration pattern typical of *T. sharmai* sp. nov. and *T. raveni*.

Etymology

The species is named after our colleague and friend Prashant Sharma, for his extensive contribution to the knowledge of the New Caledonian opiliofauna.

Troglosiro pin Giribet, Baker & Sharma sp. nov.

(Fig. 12–14)

urn:lsid:zoobank.org:act:D181F071-A3E2-4BB0-89C0-861C3F381056
Troglosiro cf. *juberthiei* (partim): Sharma & Giribet, 2009*a*.

Material examined

Holotype. Male (MNHN, ex. MCZ IZ-133875 [DNA2]) from Réserve naturelle du Pic du Pin (Pic du Pin site 1; 22°15′S, 166°49′E; 280-m elevation), Province Sud (New Caledonia), G.B. Monteith, leg., 26.xi.2004.

Paratypes. 3 males (1 mounted for SEM, 1 dissected for genitalia), 2 females, 2 juveniles (MCZ IZ-133875; ex DNA101703), same collecting data as holotype; 1 male (MCZ IZ-133854; ex DNA102343) from Réserve naturelle du Pic du Pin (–22.24713°, 166.82791°, 283-m elevation), P.P. Sharma & J.Y. Murienne, leg., 13.iv.2007, collected by sifting leaf litter; 1 male (MCZ IZ-133873; ex DNA101706) from Pic du Pin, site 1 (22°17′S, 166°50′E; 280-m elevation), G.B. Monteith, leg., 20.iv.2005, from berlesate; 1 male, 1 female (MCZ IZ-133874; ex DNA101705) from Pic du Pin, site 1 (22°15′S, 166°49′E; 280-m elevation), G.B. Monteith, leg., 21.xii.2004, from berlesate.

Additional material. 1 male, 1 female (MCZ IZ-133874; ex DNA101705) from Pic du Pin, site 1 (22°15′S, 166°49′E; 280-m elevation), G.B. Monteith, leg., 26.xi.2004.

Diagnosis

Small troglosironid with an opisthosomal depression on male sternites 4–6 and three opisthosomal gland pores located along the midline of sternite 4, the first one delimiting sternites 3 and 4, similar to those found in *T. pseudojuberthiei* sp. nov., although in the latter the first pore is the opening of two

Fig. 11. *Troglosiro sharmai* sp. nov. *A–J*, scanning electron micrographs of paratypes (MCZ IZ-151558). *A*, Male, left leg I, retrolateral view. *B*, Male, left leg II, retrolateral view. *C*, Male, left leg III, retrolateral view. *D*, Male, left leg IV, retrolateral view. *E*, Male, left tarsus I, retrolateral view. *F*, Male, left metatarsus–tarsus II, retrolateral view. *G*, Male, left metatarsus–tarsus III, retrolateral view. *H*, Male, left metatarsus–tarsus IV, retrolateral view. *I*, Female, left metatarsus–tarsus IV, retrolateral view. *J*, Male, detail of adenostyle. *K*, Light microscopy view of spermatopositor, dorsal view (MCZ IZ-151558). *L*, cLSM view of spermatopositor, dorsal view (MCZ IZ-151558).

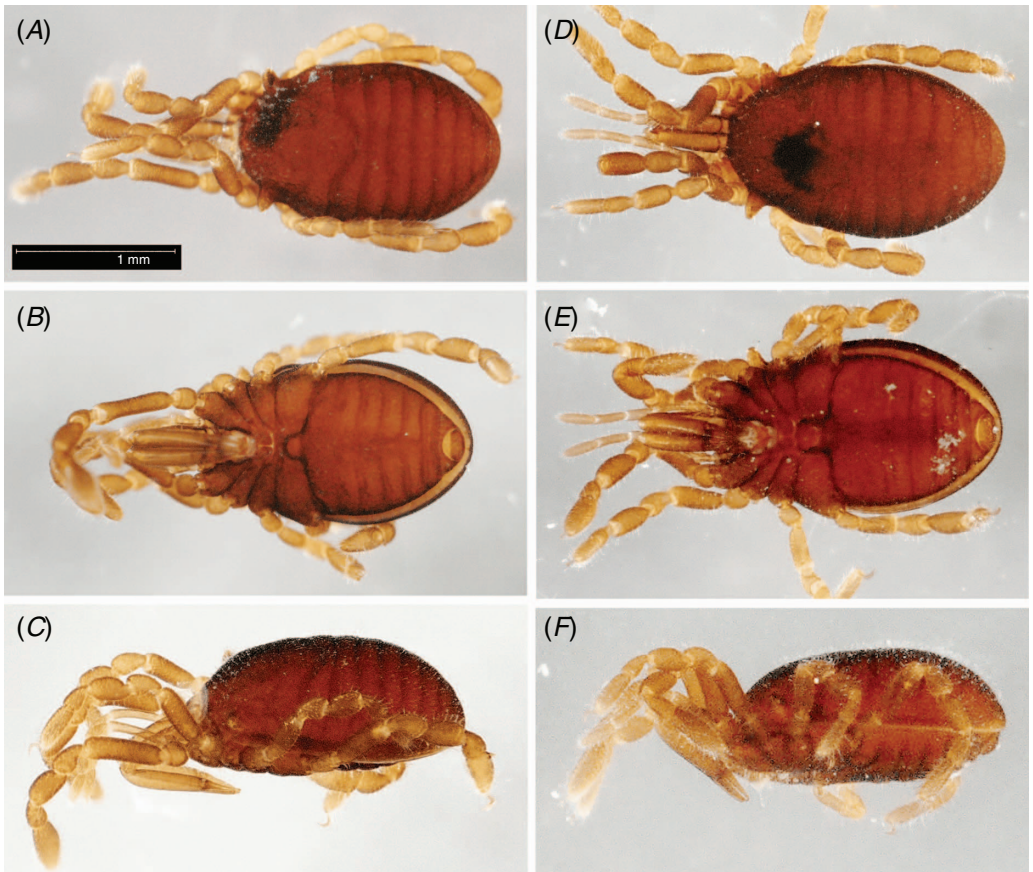

Fig. 12. *Troglosiro pin* sp. nov., stereomicroscope views of male holotype (MCZ IZ-133875) (*A–C*) and female paratype (MCZ IZ-133875) (*D–F*). *A*, Dorsal view. *B*, Ventral view. *C*, Lateral view, left side. *D*, Dorsal view. *E*, Ventral view. *F*, Lateral view, left side. Scale bar applies to all images.

close glands. Depressed opisthosomal sternites and three aligned gland pores are also found in other southern species, including *T. platnicki* and *T. ninqua*, but in these two species the pores are scattered along sternites 2, 3 and 4 (Shear 1993). *Troglosiro oscitatio* has a similar pattern for the sternal gland pores, but the opisthosomal depression is much broader and deeper, and extends to sternite 7. Other geographically close species have very different patterns of pore openings or much deeper opisthosomal sternal depressions. Spermatopositor very similar to that of *T. juberthiei* and *T. pseudojuberthiei* sp. nov., but it can be easily distinguished by the lack of ventral microtrichiae and by the enlarged movable fingers.

Description of male

Total length of male holotype 1.66 mm; width at widest point, at the third opisthosomal segment, 1.02 mm; length : width ratio 1.62; width across ozophore tips 0.91 mm. Body of a uniform reddish-brown colour (Fig. 12); legs light brown. Body surface with tuberculate–microgranulate microstructure (*sensu* Murphree 1988) across its entire surface (Fig. 13*A*).

With an opisthosomal depression on male sternites 4–6 (Fig. 13*A*); three opisthosomal sternal gland pores located along the midline of sternite 4, the first one delimiting sternites 3 and 4 (Fig. 13*C*).

All other characteristics, except when specified or measured, as in *T. sharmai* sp. nov.

Gonostome semicircular, width (110 µm) greater than length (65 µm) (Fig. 13*B*).

Spiracles in the form of a closed circle, with maximum diameter 67 µm. Anal plate without conspicuous modifications, in ventral position (Fig. 13*D*); 214 µm wide, 133 µm long.

Chelicerae (Fig. 14*A*) with a dorsal crest; with few setae. Proximal article 633 µm long, 213 µm deep, with a single posterior ventral process. Second article 807 µm long, 138 µm deep, widest near the first third of its length. Distal article 255 µm long, 52 µm deep, dentition regular.

Palp (Fig. 14*B*) without ventral process on proximal end of trochanter and without conspicuous modifications. Sparse ornamentation, in the form of small denticles, present on ventral surface and distal region of dorsal surface of trochanter. Length/width (µm) (length : width ratio in parentheses) of palpal articles from proximal to distal: 210/91 (2.3); 353/66 (2.7); remaining palp mounted for SEM broken.

Legs robust (Fig. 14*C–F*); surfaces of all trochanters, femurs, patellae, tibiae and metatarsi thickly and uniformly

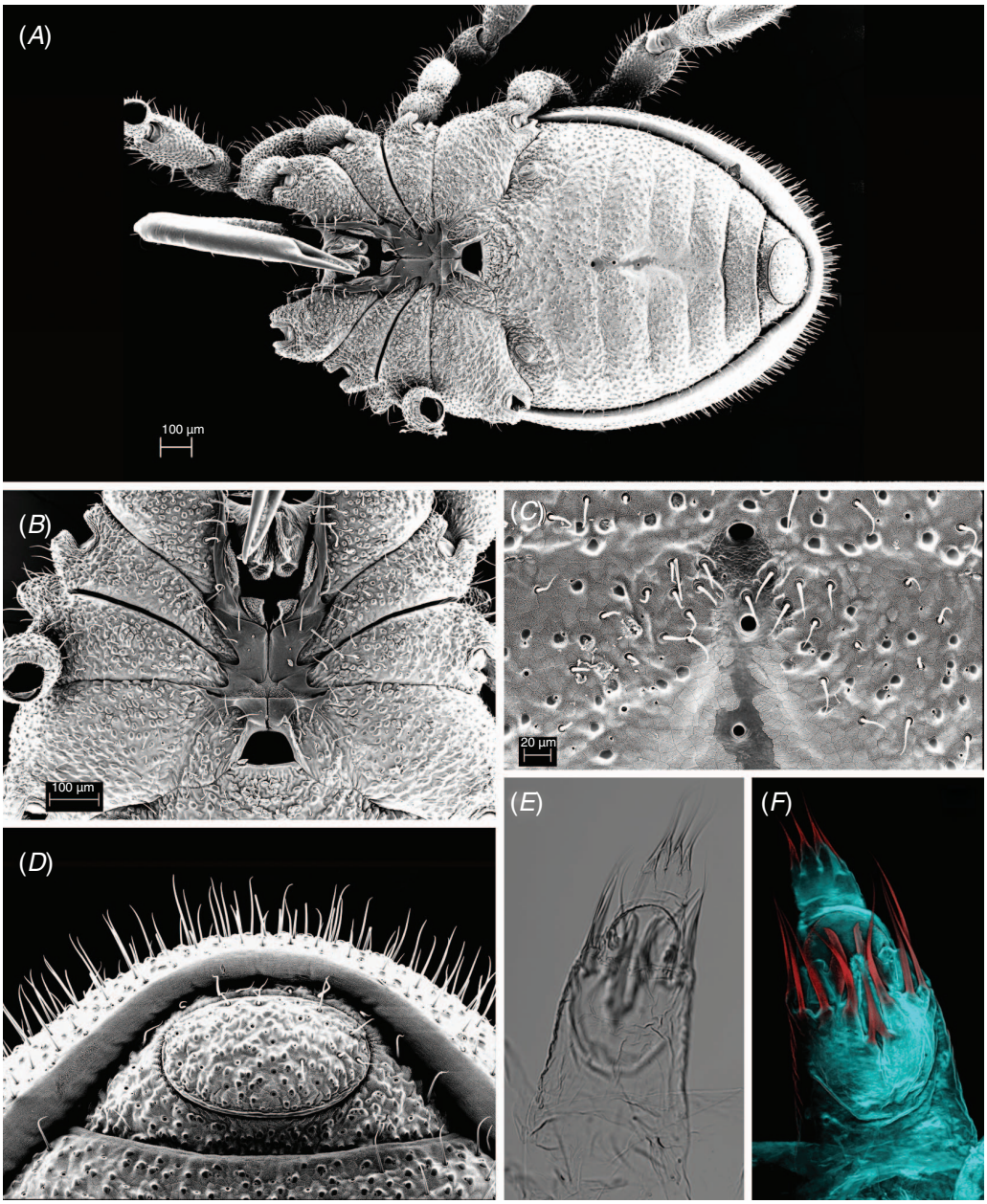

Fig. 13. *Troglosiro pin* sp. nov. *A–D*, scanning electron micrographs of male paratype (MCZ IZ-133875). *A*, Male, ventral view. *B*, Male, prosoma, sternal region. *C*, Male opisthosomal sternal region with glandular opening pores. *D*, Male, anal region. *E*, Light microscopy view of spermatopositor, dorsal view (MCZ IZ-133875). *F*, cLSM view of spermatopositor, dorsal view (MCZ IZ-133875).

granulated, except prolateral surface of trochanter IV. Tarsi not appreciably ornamented (Fig. 14*G–J*). Tarsus I with a distinct solea (Fig. 14*G*). Dorsum of tarsi I (Fig. 14*G*) and II (Fig. 14*H*) with conspicuous solenidia, trichomes and sensilla chaetica. Tarsal claw II with four teeth tapering in size from distal to proximal, with last tooth nearly imperceptible (Fig. 14*K*). For leg measurements for each article (length/maximum depth) see Table 4.

Leg formula: I > IV > II > III. Tarsus IV of male not divided, carrying a small lamelliform adenostyle proximal to most basal region of tarsus (Fig. 14*J*). Adenostyle (Fig. 14*L*) 108 µm long, curved, and pointed.

Spermatopositor (Fig. 13*E*, *F*) without ventral microtrichiae, 3 lateral microtrichiae on each side, and 4 dorsal microtrichiae, the most central pair in a much more basal position than the other ones, which are in line with the lateral microtrichiae. Ventral plate semicircular, with a rugose edge; movable fingers large, falciform, with serrated lateral margins, almost reaching the distal edge of the plate length. Four short apical microtrichiae with very enlarged bases, the

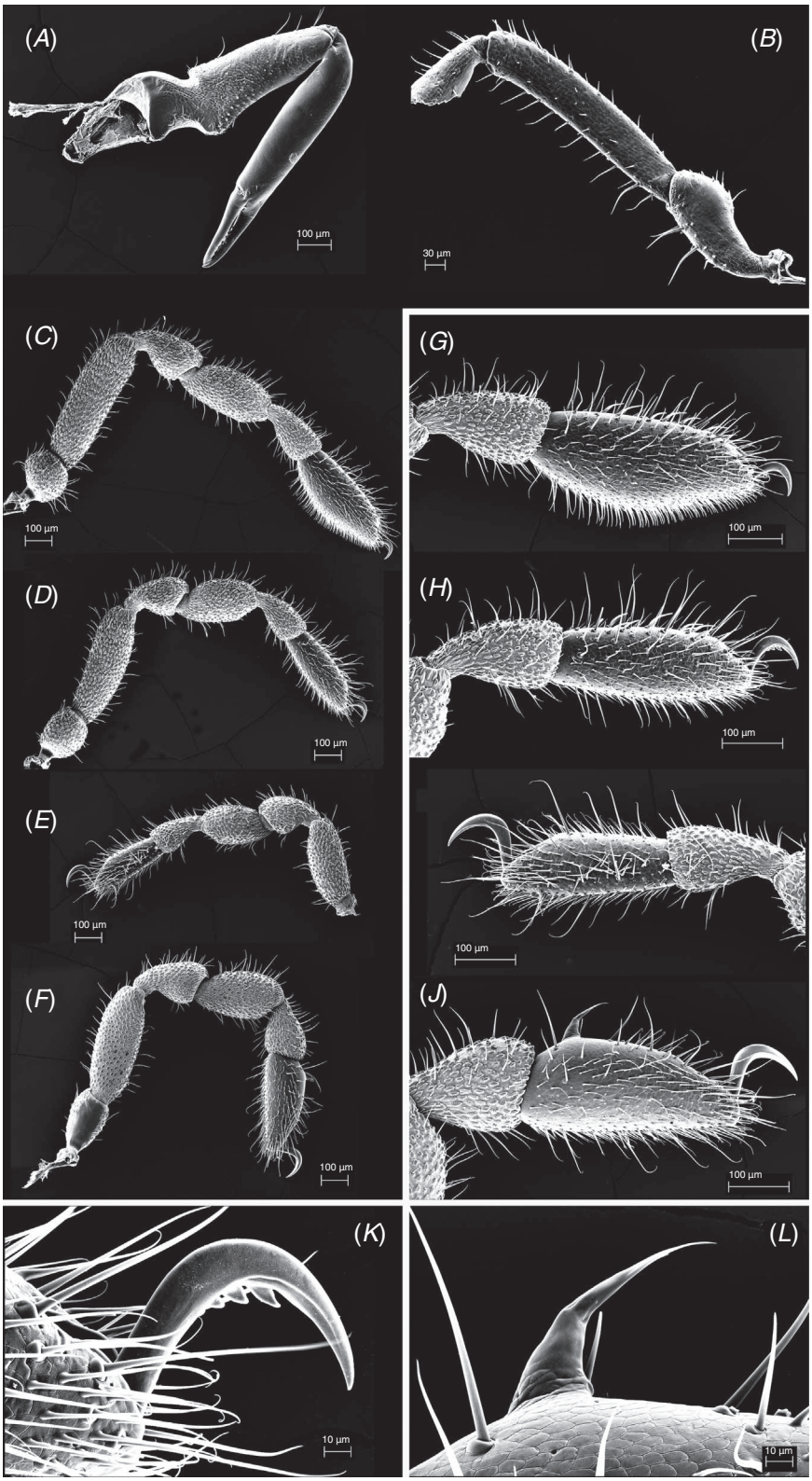

Fig. 14. *Troglosiro pin* sp. nov., scanning electron micrographs of male paratype (MCZ IZ-133875). *A*, Right chelicera, retrolateral view. *B*, Left palp, proximal articles, retrolateral view. *C*, Left leg I, prolateral view. *D*, Left leg II, prolateral view. *E*, Left leg III, retrolateral view. *F*, Left leg IV, prolateral view. *G*, Left metatarsus–tarsus I, prolateral view. *H*, Left metatarsus–tarsus II, prolateral view. *I*, Left metatarsus–tarsus III, retrolateral view. *J*, Left metatarsus–tarsus IV, retrolateral view. *K*, Left claw II. *L*, Detail of adenostyle.

Table 4. Measurements for each leg article (μm) (length/maximum depth) for *T. pin*
Tr, trochanter; Fe, femur; Pa, patella; Ti, tibia; Mt, metatarsus; Ta, tarsus; L, length. All leg measurements are in micrometres (except where specified otherwise)

	Tr	Fe	Pa	Ti	Mt	Ta	Total L (mm)
Leg I	154/192	530/168	292/169	300/171	258/137	409/180	1.943
Leg II	180/158	435/150	253/154	266/165	238/119	331/115	1.703
Leg III	91/148	304/139	237/150	211/156	209/114	290/113	1.342
Leg IV	229/146	414/168	283/168	292/179	234/159	357/157	1.809

four bases together being almost as broad as the ventral plate; apical microtrichiae extend well beyond ventral plate and lateral microtrichiae.

Description of female

Total length of female paratype (Fig. 12*D–F*) 1.76 mm; width at widest point 1.09 mm; length : width ratio 1.61; width across ozophores 0.99 mm. Anal plate 225 × 120 μm. All other characteristics as in *T. sharmai* sp. nov. Ovipositor not studied.

Distribution

Known only from a few collections in a few nearby sites at the Réserve naturelle du Pic du Pin.

Remarks

As discussed above, *T. pin* sp. nov. was previously considered as part of the variation of *T. juberthiei* by Sharma (2006) and Sharma and Giribet (2009*a*), although recognising that it could constitute a cryptic species. However, they did not consider that this species could be distinct from the other species described here, *T. pseudojuberthiei* sp. nov.

Etymology

The species is named after its type locality, the Réserve naturelle du Pic du Pin.

Troglosiro pseudojuberthiei Giribet, Baker & Sharma sp. nov.

(Fig. 1*E*, *F*, 15–17)

urn:lsid:zoobank.org:act:27F59FDB-4F98-4549-A309-6328DABEBAF8
Troglosiro cf. *juberthiei* (partim): Sharma & Giribet, 2009*a*.

Material examined

Holotype. Male (MNHN, ex. MCZ IZ-133855; ex DNA102344) from Réserve Speciale Botanique du Pic du Grand Kaori/Grand Lac (–22.27961°, 166.89455°, 254-m elevation), Province Sud (New Caledonia), J.Y. Murienne & P.P. Sharma, leg., 17.iv.2007, collected by sifting leaf litter.

Paratypes. 1 female (MCZ IZ-133855; ex DNA102344), same collecting data as holotype. 2 males, 6 females (MCZ IZ-151618) from Réserve Speciale Botanique du Pic du Grand Kaori/Grand Lac (–22.27977°, 166.89454°, 251-m elevation), Province Sud (New Caledonia), C.M. Baker & G. Giribet, leg., 18.xi.2018, collected by sifting leaf litter. 6 males (1 dissected for genitalia, 1 mounted for SEM), 2 females, 2 juveniles (MCZ IZ-133859, ex DNA101691) from Pic du Grand Kaori (Monteith site 2: 22°17′S, 166°54′E), Province Sud (New Caledonia), G.B. Monteith, leg., 20.iv.2005. 4 males (1 dissected for genitalia), 5 females (MCZ IZ-133868; ex DNA101697) from Forêt Nord (Kwa Neie) (Monteith site 2: 22°19′23″S, 166°54′55″E, 200-m elevation), Province Sud (New Caledonia), G.B. Monteith & P. Grimbacher, leg., 2–4.xii.2004, berlesate.

Additional material. 1 juvenile preserved in RNA*later*, transferred to MCZ cryo-collection (MCZ IZ-151618), same collecting data as holotype; 1 juvenile preserved in RNA*later* (MCZ IZ-151618) used to sequence its transcriptome (SRR11812288), same collecting data as holotype. 1 juvenile (MCZ IZ-133856; ex DNA102345) from Pic du Grand Kaori (–22.27961°, 166.89455°, 254-m elevation), Province Sud (New Caledonia), J.Y. Murienne & P.P. Sharma, leg., 17.iv.2007, collected by sifting leaf litter. 1 male (MCZ IZ-133860, ex DNA101692) from Pic Du Grand Kaori (22°17′S, 166°54′E), Province Sud (New Caledonia), G.B. Monteith, leg., 21.xi.2001, hand collected. 1 female (MCZ IZ-133861, ex DNA101689) from Pic du Grand Kaori (Monteith site 2: 22°17′S, 166°53′E), Province Sud (New Caledonia), G.B. Monteith & P. Grimbacher, leg., 2.xii.2004, collected by intercept trap. 1 male (MCZ IZ-133862, ex DNA101690) from Pic du Grand Kaori (Monteith site 1: 22°17′S, 166°53′E), Province Sud (New Caledonia), G.B. Monteith & P. Grimbacher, leg., 22.xi.2004, berlesate. Multiple specimens (MCZ IZ-133863, ex DNA101692) from Pic du Grand Kaori (Monteith site 2: 22°17′S, 166°53′E), Province Sud (New Caledonia), G.B. Monteith & P. Grimbacher, leg., 22.xi.2004, berlesate. Multiple specimens (MCZ IZ-133864, ex DNA101694) from Pic du Grand Kaori (Monteith site 1: 22°17′S, 166°53′E, 250-m elevation), Province Sud (New Caledonia), G.B. Monteith & P. Grimbacher, leg., 22.xi.2004, berlesate. 1 juvenile (MCZ IZ-133865, ex DNA101693) from Pic du Grand Kaori (Monteith site 1: 22°17′S, 166°53′E), Province Sud (New Caledonia), G.B. Monteith, leg., 22.xii.2004, berlesate. 1 female (MCZ IZ-133867; ex DNA101699) from Forêt Nord (Kwa Neie) (Monteith site 1: 22°19′S, 166°55′E, 480-m elevation), Province Sud (New Caledonia), G.B. Monteith, leg., 1–2.xii.2004. 1 female (MCZ IZ-133869; ex DNA101700) from Forêt Nord (Kwa Neie) (Monteith site 2: 22°19′23″S, 166°54′55″E, 210-m elevation), Province Sud (New Caledonia), G.B. Monteith, leg., 2.xii.2004, hand collecting. Multiple specimens (MCZ IZ-133870; ex DNA101701) from Forêt Nord (Kwa Neie) (Monteith site 2: 22°19′23″S, 166°54′55″E, 210-m elevation), Province Sud (New Caledonia), G.B. Monteith, leg., 21.iv.2005, berlesate. 2 males (MCZ IZ-133871; ex DNA101698) from Forêt Nord (Kwa Neie) (Monteith site 1: 22°19′S, 166°55′E, 480-m elevation), Province Sud (New Caledonia), G.B. Monteith, leg., 22.xii.2004. 1 female (MCZ IZ-133872; ex DNA101702) from Forêt Nord (Kwa Neie) (Monteith site 2: 22°19′26″S, 166°54′52″E, 200-m elevation), Province Sud (New Caledonia), G.B. Monteith, leg., 22.xii.2004, berlesate. 22 specimens (MCZ IZ-133857, ex DNA102346) from Forêt Nord (Kwa Neie) (–22.32291°, 166.91505°, 197-m elevation), Province Sud (New Caledonia), J.Y. Murienne & P.P. Sharma, leg., 17.iv.2007, collected by sifting leaf litter.

Diagnosis

Small troglosironid with an opisthosomal depression on male sternites 4–6 and three opisthosomal gland pores located along the midline of sternite 4, the first one with a double pore that delimits sternites 3 and 4, similar in configuration to *T. pin* sp.

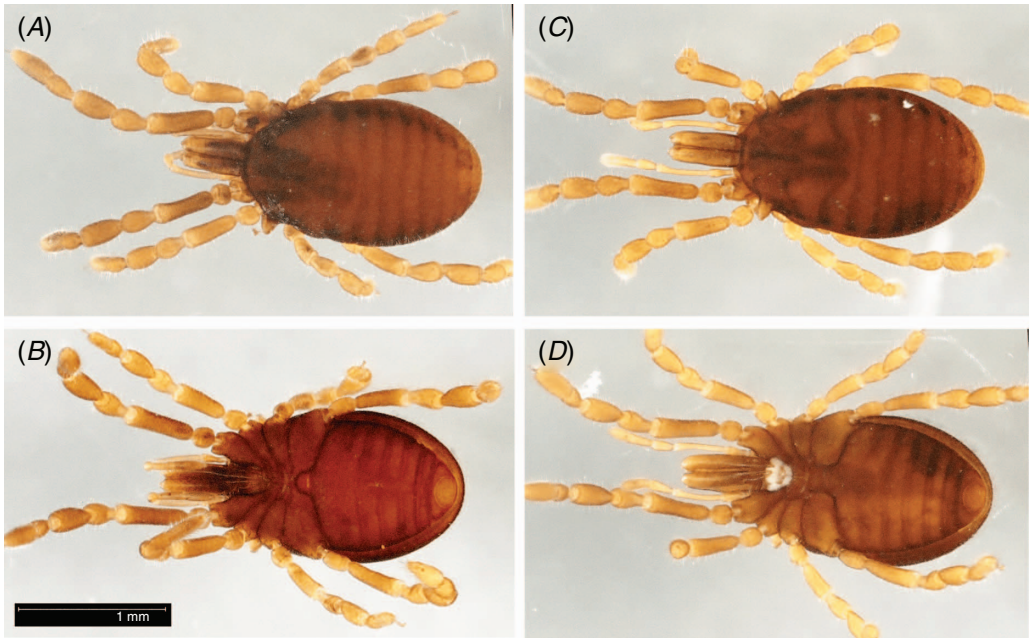

Fig. 15. *Troglosiro pseudojuberthiei* sp. nov., stereomicroscope views of male holotype (MCZ IZ-151618) (*A*, *B*) and female paratype (MCZ IZ-151618) (*C*, *D*). *A*, Dorsal view. *B*, Ventral view. *C*, Dorsal view. *D*, Ventral view. Scale bar applies to all images.

nov., although in the latter the first pore is not paired. Depressed opisthosomal sternites and three aligned gland pores are also found in other southern species, including *T. platnicki* and *T. ninqua*, but in these two species the pores are scattered along sternites 2, 3 and 4 (Shear 1993). *Troglosiro oscitatio* has a similar pattern for the sternal gland pores, but the opisthosomal depression is much broader and deeper, and extends to sternite 7. Other geographically close species have very different patterns of pore openings or much deeper opisthosomal sternal depressions. Gonostome more elongated than in *T. pin* sp. nov. Spermatopositor very similar to that of *T. juberthiei* and *T. pin* sp. nov., but it can be distinguished by the very enlarged bases of the apical microtrichiae, which are almost as broad as the ventral plate, unlike in *T. juberthiei* (Shear 1993, fig. 24–25) and unlike *T. pin* sp. nov, it has ventral microtrichiae.

Description of male

Total length of male holotype 1.62 mm; width at widest point, at the third opisthosomal segment, 1.01 mm; length : width ratio 1.60; width across ozophore tips 0.89 mm. Body of a uniform reddish-brown colour (Fig. 15); legs light brown–yellow. Body surface with tuberculate–microgranulate microstructure (*sensu* Murphree 1988) across its entire surface (Fig. 16*A*).

With an opisthosomal depression on male sternites 4–6 (Fig. 16*A*, *C*, *D*), delimiting an area with sparser granulation; three opisthosomal sternal gland pores located along the midline of sternite 4, the first one with a double pore opening (Fig. 16*C*, *D*).

All other characteristics, except when specified or measured, as in *T. sharmai* sp. nov. and *T. pin* sp. nov., the latter being a very similar species.

Gonostome semicircular, width (112 µm) greater than length (75 µm) (Fig. 16*B*).

Anal plate without conspicuous modifications; in ventral position (Fig. 16*E*); 236 µm wide, 114 µm long.

Chelicerae (Fig. 17*A*) with a dorsal crest; with few setae. Proximal article 667 µm long, 228 µm deep, with a single posterior ventral process. Second article 853 µm long, 133 µm deep, almost cylindrical for most of its length. Distal article 251 µm long, 55 µm deep, dentition regular.

Palp (Fig. 17*B*) without ventral process on proximal end of trochanter; without conspicuous modifications, and very sparse ornamentation, in the form of small denticles, present on trochanter only. Length : width (µm) (length : width ratio in parentheses) of palpal articles from trochanter to tarsus: 196/93 (2.1); 366/67 (5.4); 193/69 (2.8); 264/68 (3.9); 253/71 (3.5); total length 1.27 mm. Palpal claw 52 µm long.

Legs robust (Fig. 17*C–F*); surfaces of all trochanters, femurs, patellae, tibiae and metatarsi thickly and uniformly granulated. Tarsi not appreciably ornamented (Fig. 17*G–J*). Tarsus I with a distinct solea (Fig. 17*G*). Dorsum of tarsi I (Fig. 17*G*) and II (Fig. 17*H*) with conspicuous solenidia, trichomes and sensilla chaetica. Tarsal claw II with four teeth tapering in size from distal to proximal (Fig. 17*L*). For leg measurements for each article (length/maximum depth) in see Table 5.

Leg formula: I > IV > II > III. Tarsus IV of male not divided, carrying a small lamelliform adenostyle proximal to most basal region of tarsus (Fig. 17*J*). Adenostyle subtriangular, although the imaged one is probably broken (Fig. 17*K*).

Spermatopositor (Fig. 16*F*, *G*) with three ventral microtrichiae with enlarged bases, two lateral microtrichiae on each side, similar to ventral ones in length (Fig. 16*G*), and

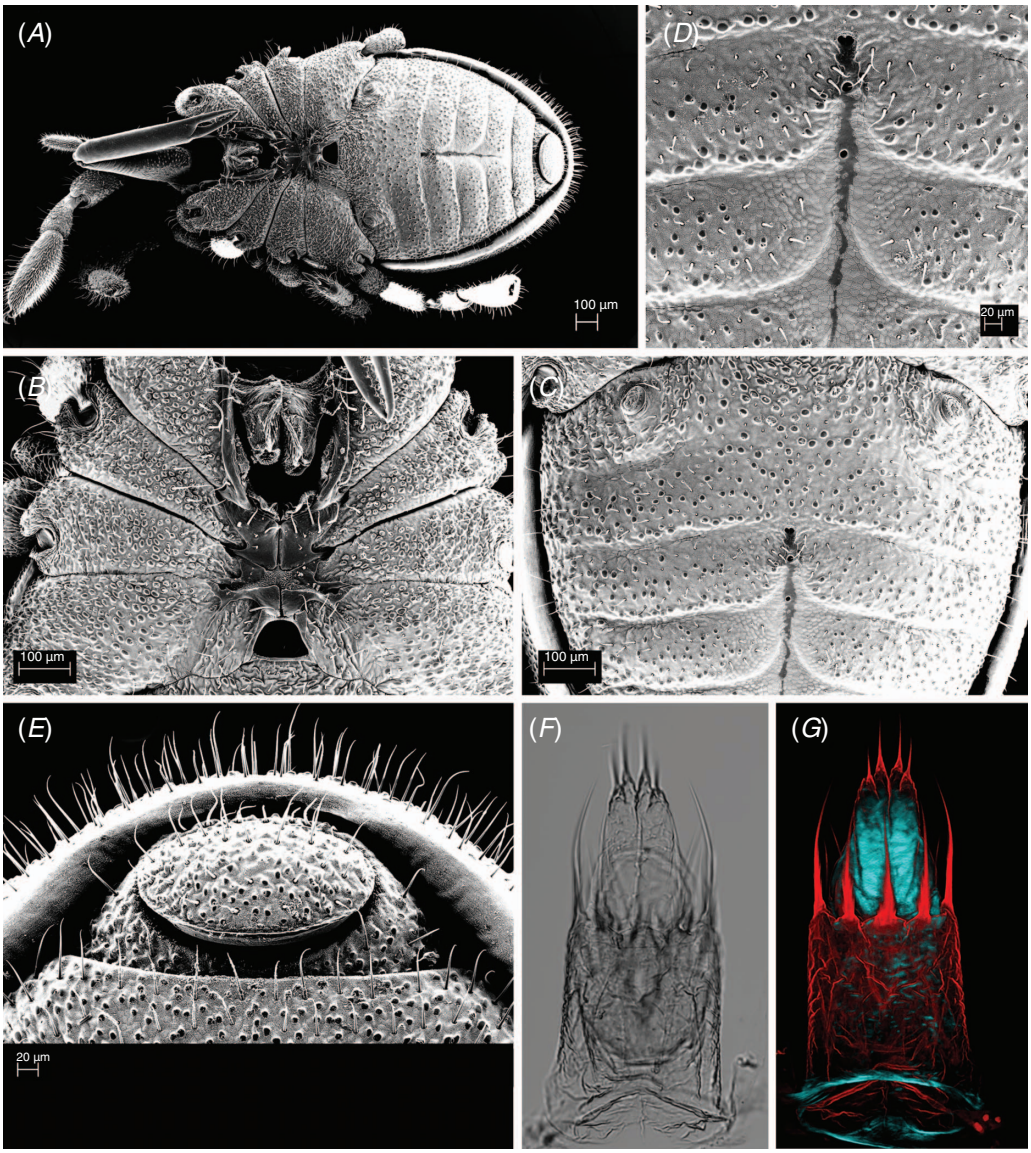

Fig. 16. *Troglosiro pseudojuberthiei* sp. nov. *A–E*, scanning electron micrographs of male paratype (MCZ IZ-133859). *A*, Ventral view. *B*, Prosoma, sternal region. *C*, Opisthosomal sternal region with glandular opening pores. *D*, Detail of opisthosomal glandular opening pores. *E*, Anal region. *F*, Light microscopy view of spermatopositor, ventral view (MCZ IZ-133859). *G*, cLSM view of spermatopositor, ventral view (MCZ IZ-133859).

4 dorsal microtrichiae, forming a V. Ventral plate semicircular, with a rugose edge; movable fingers enlarged, falciform, reaching about half of the plate length and with serrated lateral margins. Four short apical microtrichiae with enlarged scaly bases, extending well beyond both the ventral plate and the ventral, lateral and dorsal microtrichiae.

Description of female

Total length of female paratype (Fig. 12*C*, *D*) 1.66 mm; width at widest point 1.03 mm; length : width ratio 1.61; width across ozophores 0.88 mm. Anal plate 207 × 142 µm. All other characteristics as in *T. sharmai* sp. nov. and *T. pin* sp. nov. Ovipositor not studied.

Distribution

Known from multiple collections in several sites from two nearby forest reserve areas (Réserve naturelle du Pic du Grand Kaori and Réserve naturelle de la Forêt Nord) and their surroundings.

Remarks

As discussed above, *T. pseudojuberthiei* sp. nov. was previously considered as part of the variation of *T. juberthiei* by Sharma (2006) and Sharma and Giribet (2009*a*), although recognising that it could constitute a cryptic species. However, in this study we showed that this species is different from *T. pin* sp. nov., which was also

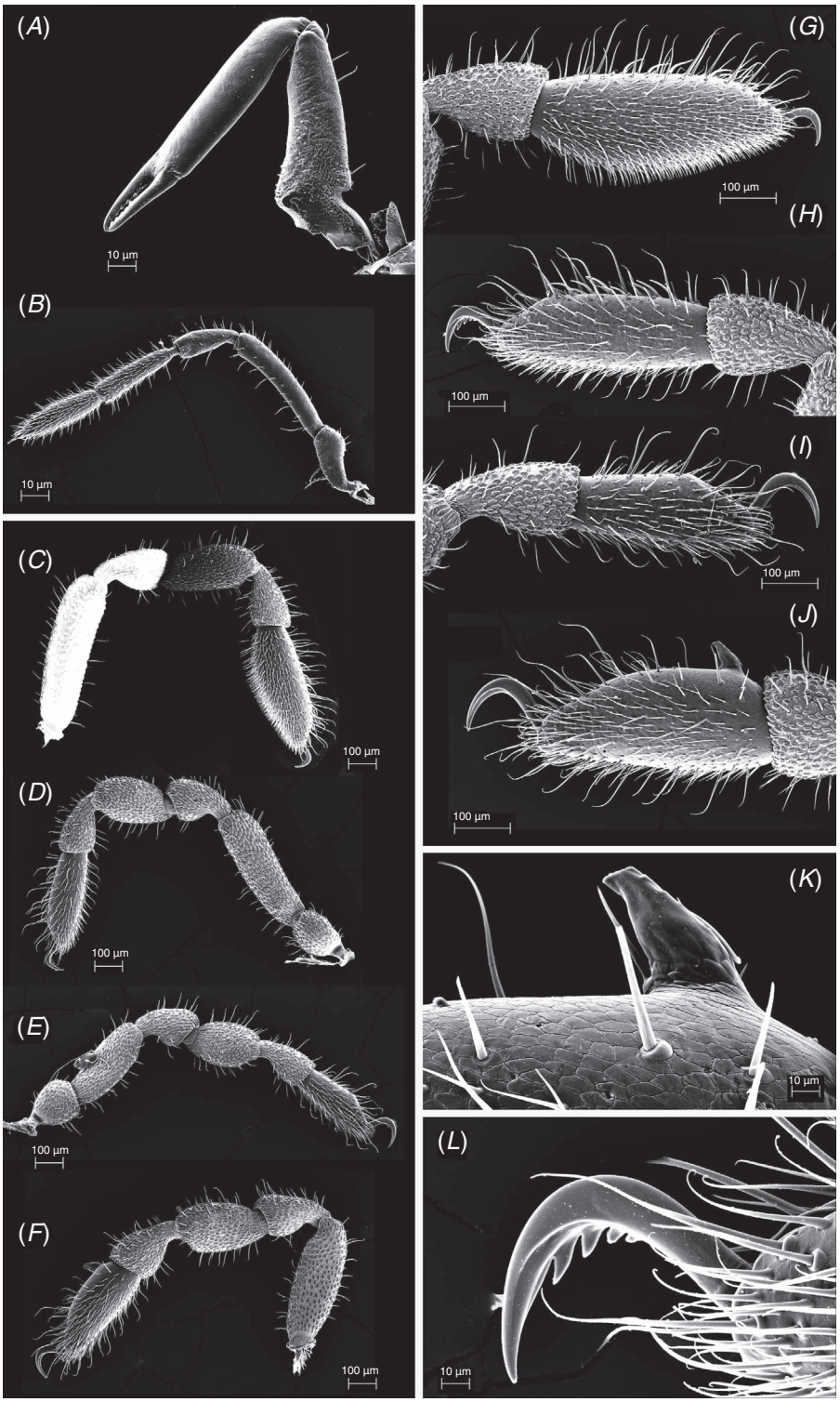

Fig. 17. *Troglosiro pseudojuberthiei* sp. nov., scanning electron micrographs of male paratype (MCZ IZ-133859). *A*, Left chelicera, retrolateral view. *B*, Left palp, retrolateral view. *C*, Left leg I, prolateral view. *D*, Left leg II, retrolateral view. *E*, Left leg III, prolateral view. *F*, Left leg IV, retrolateral view. *G*, Left metatarsus–tarsus I, prolateral view. *H*, Left metatarsus–tarsus II, retrolateral view. *I*, Left metatarsus–tarsus III, prolateral view. *J*, Left metatarsus–tarsus IV, retrolateral view. *K*, Detail of adenostyle. *L*, Left claw II.

Table 5. Measurements for each leg article (μm) (length/maximum depth) for *T. pseudojuberthiei*
Tr, trochanter; Fe, femur; Pa, patella; Ti, tibia; Mt, metatarsus; Ta, tarsus; L, length. All leg measurements are in micrometres (except where specified otherwise)

	Tr	Fe	Pa	Ti	Mt	Ta	Total L (mm)
Leg I	129/–	562/162	282/164	335/163	247/147	446/179	2.001
Leg II	177/138	450/146	249/162	255/163	238/131	348/114	1.717
Leg III	176/159	315/139	238/151	233/167	221/120	298/113	1.481
Leg IV	188/–	462/168	285/162	294/185	269/175	386/172	1.884

included as *T.* cf. *juberthiei* in the earlier studies. *Troglosiro pin* sp. nov. is known only from the Réserve naturelle du Pic du Pin, whereas *T. pseudojuberthiei* sp. nov. occurs in two nearby but isolated reserves. Considering the presence of similar habitat in other nearby forests and the possibility that *Troglosiro* sp. IZ-134784 from Col de Yaté is an unidentified specimen of *T. pin* sp. nov. (see above), this area emerges as an interesting one to study speciation among closely related short-range endemics.

Etymology

The specific epithet refers to the original confusion of this species with *Troglosiro juberthiei*.

Troglosiro dogny Giribet & Baker sp. nov.

(Fig. 1*C*, *D*, 18)

urn:lsid:zoobank.org:act:55BA2C61-0AAD-4342-A008-45FBA61E41CD

Material examined

Holotype. Male (MNHN, ex. MCZ IZ-151570; 1 leg used for DNA extraction) from Plateau de Dogny (–21.61696°, 165.88393°, 914-m elevation), Sarraméa, Province Sud (New Caledonia), C.M. Baker & G. Giribet, leg., 13.xi.2018, collected by sifting leaf litter.

Paratype. 1 female (MCZ IZ-151570; 1 leg used for DNA extraction), same collecting data as holotype.

Additional material. 1 juvenile (MCZ IZ-51947; ex. Queensland Museum NC25-008; ex. MCZ DNA101588) in 70% EtOH used for DNA work, only part of the exoskeleton left; from Plateau de Dogny (21°37′15″S, 165°52′40″E, 950-m elevation), C.J. Burwell, leg., 16.xi.2002.

Diagnosis

Troglosironid with a broad depression of opisthosomal sternites, extending from end of sternite 2 to the end of 7 (Fig. 18*C*, *G*), with 3 sternal gland pore openings on the anterior end of sternite 3, 4 and 5, similar to *T. ninqua* and *T. oscitatio*. *Troglosiro pin* sp. nov. also presents three gland openings, but they all are concentrated in sternite 4. *Troglosiro dogny* sp. nov. is easily distinguished from all other *Troglosiro* species by the two pairs of pale patches seen on the dorsum, on opisthosomal tergites I and II, the posterior pair much larger, both when alive (Fig. 1*C*, *D*) and when preserved in ethanol (Fig. 18*A*).

Description of male

Total length of male holotype 2.03 mm; width at widest point, at the third opisthosomal segment 1.29 mm; length : width ratio 1.57; width across ozophore tips 1.22 mm. Body reddish-brown with distinct lighter patches of colouration on the dorsum, on opisthosomal tergites 1 and 2 (Fig. 1*C*, *D*, 18*A*). Body surface with tuberculate–microgranulate microstructure (*sensu* Murphree 1988) across its entire surface.

Gonostome semicircular, width (177 μm) greater than length (116 μm) (Fig. 18*E*). Anal plate without conspicuous modifications; in ventral position (Fig. 18*G*); 274 μm wide, 174 μm long. Opisthosomal sternal region with a broad depression, extending from end of sternite 2 to the end of 7 (Fig. 18*C*, *G*), with 3 sternal gland pore openings on the anterior end of sternite 3, 4 and 5.

All other characteristics as in *T. sharmai* sp. nov. described above, except where indicated. Spermatopositor not studied.

Description of female

Total length of female paratype 2.14 mm; width at widest point 1.33 mm; length : width ratio 1.60; width across ozophores 1.24 mm. Body reddish-brown with distinct lighter patches of colouration on the dorsum, on opisthosomal tergite 2 (Fig. 1*C*, left). Anal plate 290 × 190 μm. All other characteristics as in *T. sharmai* sp. nov. Ovipositor not studied.

Distribution

Known only from two collections from Plateau de Dogny, above 900-m elevation.

Remarks

This species was first collected in 2002, but the only specimen known at the time was a juvenile. This specimen prompted us to search for this species during our 2018 expedition, resulting in one male and one female specimen, used for this species description. Although the species description is not as detailed as the other ones we typically produce, we preferred to preserve the specimens nearly intact for the time being, instead of mounting them for SEM and dissecting them for genitalia. Its morphological characters and phylogenetic position were deemed sufficient for establishing this new taxon, especially due to its extreme isolation, found only on the plateau and not in any of the forests we searched below 900 m. Phylogenetically, this species is not closely related to the three geographically closest species, *T. monteithi*, *T. oscitatio* and the undescribed species from Mount Do (see Fig. 2–6). Additional details for this species can be added in the future if more specimens become available.

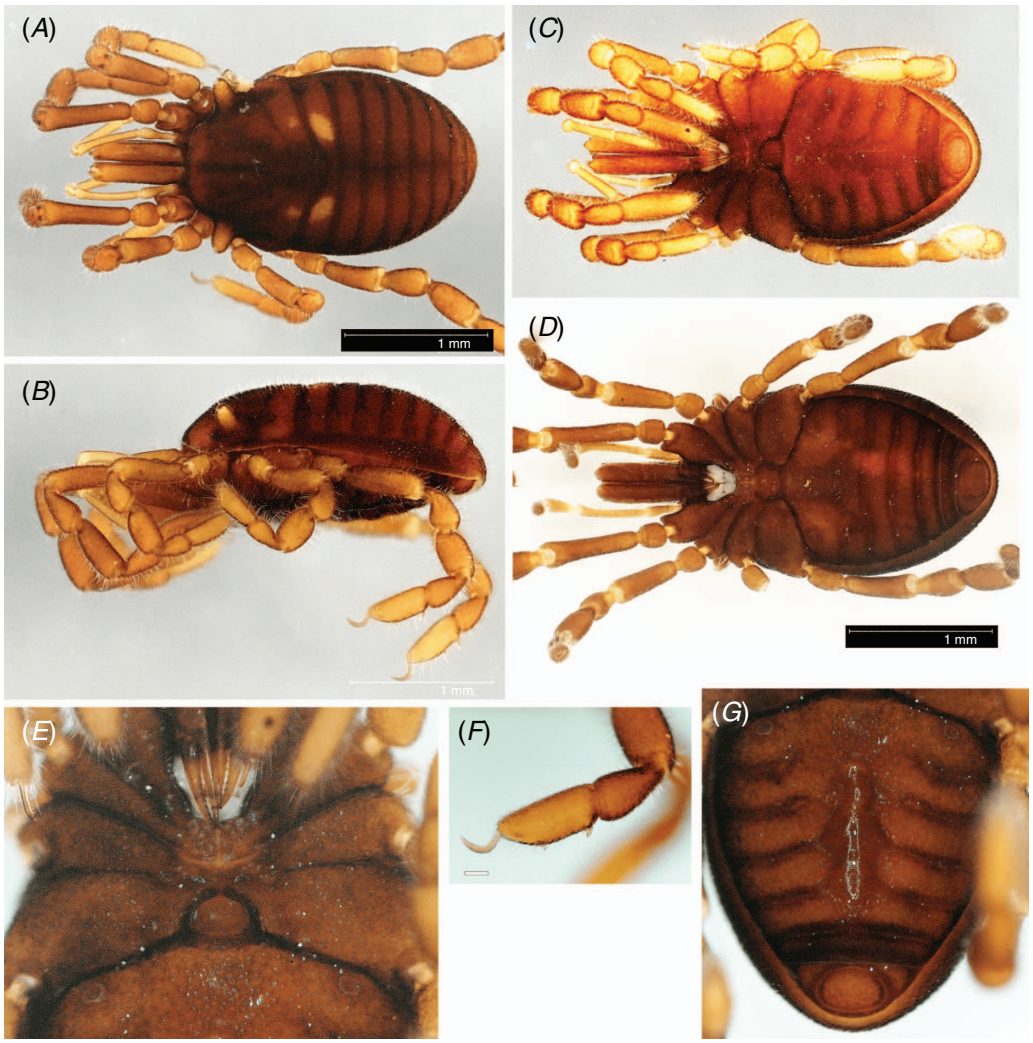

Fig. 18. *Troglosiro dogny* sp. nov., stereomicroscope views of male holotype (MCZ IZ-151570) (*A–C*, *E–G*) and female paratype (MCZ IZ-151570) (*D*). *A*, Male, dorsal view. *B*, Male, lateral view. *C*, Male, ventral view. *D*, Female, ventral view. *E*, Male, prosomal sternal region. *F*, Male, detail of left leg IV, prolateral view (scale bar, 100 μm). *G*, Male, opisthosomal sternal region with depression for sternal opisthosomal glands.

Etymology

The species is named after its type locality, an emblematic mountain of New Caledonia that served as a place for exchange between the tribes from the East and the West of Grande Terre.

A key to the males of *Troglosiro*

1a. *Troglosiro* without a male opisthosomal sternal depression 2
1b. *Troglosiro* with a male opisthosomal sternal depression 6
2a. Without a cheliceral dorsal crest 3
2b. With a cheliceral dorsal crest 5
3a. With two opisthosomal sternal pores along midline 4
3b. With four opisthosomal sternal pores along midline .... *T. tillierorum*
4a. With a banded pigmented pattern on dorsum and venter..... ..... *T. sharmai* sp. nov.
4b. Uniform light colouration ..... *T. aelleni*
5a. With a banded pigmented pattern; with four opisthosomal sternal pores along midline ..... *T. raveni*
5b. Without pigmented pattern; with three opisthosomal sternal pores along midline ..... *T. sheari*
6a. With a single longitudinal depression of opisthosomal sternites 7
6b. With a double longitudinal depression of opisthosomal sternites..... ..... *T. monteithi*
7a. With an anterior semicircular field of opisthosomal sternal pores..... .....*T. wilsoni*
7b. With anterior opisthosomal sternal pores forming a separate pair..... 8
7c. With all opisthosomal sternal pores along midline 9
8a. With a broad sternal depression, more than half the width of opisthosoma, with only two pores, forming a pair .... *T. longifossa*
8b. With a narrow sternal depression, with four sternal pores, the first forming a pair .....*T. urbanus*
9a. With a small opisthosomal sternal depression (limited to sternites 4–5), with two pores.....*T. brevifossa*
9b. With three opisthosomal sternal pores and large opisthosomal depression 10
10a. With a dorsal colouration pattern with two pairs of lighter spots on opisthosomal tergites I and II .....*T. dogny* sp. nov.

10b. With a distinct dorsal M-shaped colouration pattern ..... *T. oscitatio*
10c. Without distinct dorsal colouration patterns.....11
11a. Large species, more than 2 mm long..... *T. ninqua*
11b. Small species, less than 1.8 mm long.....12
12a. With three opisthosomal sternal gland pores on sternite 4 13
12b. With two or three opisthosomal sternal gland pores, not circumscribed to sternite 4..... 14
13a. Spermatopositor with ventral microtrichiae and enlarged bases of the apical microtrichiae..... *T. pseudojuberthiei* sp. nov.
13b. Spermatopositor without ventral microtrichiae and enlarged movable fingers..... *T. pin* sp. nov.
14a. With two opisthosomal sternal pores.....*T. juberthiei*
14b. With three sternal opisthosomal pores ..... *T. platnicki*

Taxonomic discussion and concluding remarks

A synapomorphy of Sternophthalmi is the presence of exocrine gland openings in the anterior opisthosomal sternal region of males in all troglosironids, all ogoveids, and most neogoveids, as opposed to the other Cyphophthalmi families where the opisthosomal exocrine glands, when present, open in the posterior opisthosomal tergites (Giribet *et al*. 2012). However, almost nothing is known about the anatomy of these opisthosomal glands. In Troglosironidae, these open by pores along the opisthosomal midline, often associated to sternites 2, 3, 4 or 5. The opisthosomal glands are actually paired and symmetrical, their conduits often joining along the midline (see Shear 1993, fig. 30). In some species, however, these glands present as paired separate openings (e.g. *T. longifossa*, see Sharma and Giribet 2005, fig. 11; *T. urbanus*, see Sharma and Giribet 2009*b*, fig. 108) or as multiple openings that traverse the midline (in *T. wilsoni*, see Sharma and Giribet 2009*b*, fig. 46). These openings were first described by Juberthie (1979) as 'medio-ventral glands', the anteriormost probably with two close openings (see Juberthie 1979, fig. 2D), as in *T. sharmai* sp. nov. (Fig. 9*D*) and *T. pseudojuberthiei* sp. nov. (Fig. 16*D*). Shear (1993) called them 'median exocrine glands' and Giribet and Boyer (2002) referred to them as 'male sternal glands' (their character 22), at the time failing to recognise a possible homology to the anal glands of sironids, stylocellids and pettalids, as in subsequent data matrices (de Bivort and Giribet 2004).

Homology of the sternal glands of Troglosironidae and Neogoveidae to the anal glands found in some Pettalidae, Sironidae, and Stylocellidae was first proposed by Juberthie (1979), and later on by Sharma and Giribet (2005), although Juberthie (1979) did not consider homology to the sternal gland openings of Neogoveidae and Ogoveidae. Boyer and Giribet (2007: characters 32, 33) explicitly homologised all opisthosomal glands, irrespective of whether they open on the sternal region or on the posterior tergites or anal region.

In troglosironids, when more than two gland pore openings exist, the posterior ones tend to be smaller and sometimes difficult to observe, even under SEM, as they may be obscured by secretions of the pores. Therefore, it is likely that some of the published descriptions have mischaracterised these gland openings. Micro-CT scanning may one day help understand these sexually dimorphic organs across Cyphophthalmi.

In this study we revisited the phylogeny of Troglosironidae, assessed the current taxonomic diversity of the group, and described four species that can be distinguished by a combination of morphological and molecular characters. The shelf life of these species spans from 2 to 19 years, well below the average for terrestrial animals and within the range of invertebrates. Our work brings the *Troglosiro* described species count up to 17, a considerable number for a group whose first species was described in 1979. It also continues to highlight their extreme condition of short-range endemism, as shown in other Cyphophthalmi (e.g. Fernández and Giribet 2014; Clouse *et al*. 2016; Schwentner and Giribet 2018), with these animals representing especially vulnerable elements of our biodiversity, and thus potentially ineluctable for conservation priority (Harvey *et al*. 2011). Given that New Caledonia is considered one of the areas with the most endangered forests in the world, ranked second only after Indo-Burmese forests according to Conservation International, and a hotspot for conservation priority (Myers *et al*. 2000), assessing its short-range endemic fauna could be used as an indicator of the state of conservation of its biodiversity.

Conflicts of interest

G. Giribet is the Editor-in-Chief and P. P. Sharma is an Associate Editor of *Invertebrate Systematics*. Despite this relationship, they took no part in the review and acceptance of this manuscript. The authors declare that they have no further conflicts of interest.

Declaration of funding

Field work in 2007 was supported by the Goelet Award, the Kalathia Family Trust, and the Exploration Fund to P. P. Sharma. Field work in 2018 was funded by a Putnam Expedition Grant from the MCZ to C. M. Baker This research was supported by NSF Grants DEB-1754278 and DEB-1457539 to G. Giribet.

Acknowledgements

We are indebted to Geoff Monteith for sending us his extensive collections of New Caledonian Cyphophthalmi, as well as Jean-Jérôme Cassan at the Direction du Développement Économique et de l'Environnement for assisting with permits (number 609011 – 75/2018/DEPART/JJC) and field work logistics. Martin Brinkert (DDEE) and Marcelin Jereureu-Gowé (chef, tribu d'Ouendji) further assisted with field logistics in New Caledonia. Additional permits for the Province Sud for the 2007 collections were provided by David Paulaud (number 6024 –1549/DENV/MT/DP) and for the 2018 expedition by Philippe Bouchet (number 1980-2018/ARR/DENV). Associate Editor Mark Harvey and two anonymous reviewers provided comments on an earlier version of this manuscript. We dedicate this work to our colleague and friend Norman I. Platnick, who influenced arachnology of New Caledonia, and who sadly left us during the conclusion of this research.

References

Abadi, M., Barham, P., Chen, J., Chen, Z., Davis, A., Dean, J., Devin, M., Ghemawat, S., Irving, G., Isard, M., Kudlur, M., Levenberg, J., Monga, R., Moore, S., Murray, D. G., Steiner, B., Tucker, P., Vasudevan, V., Warden, P., Wicke, M., Yu, Y., Zheng, X., and Brain, G. (2016). TensorFlow: a system for large-scale machine learning. In '12th USENIX Symposium on Operating Systems Design and Implementation (OSDI '16)', 2–4 November 2016, Savannah, GA, USA.) pp. 265–283. (USENIX Association.) Available at https://www.usenix.org/system/files/conference/osdi16/osdi16-abadi.pdf [Verified 22 August 2020].

Boyer, S. L., and Giribet, G. (2007). A new model Gondwanan taxon: systematics and biogeography of the harvestman family Pettalidae (Arachnida, Opiliones, Cyphophthalmi), with a taxonomic revision of genera from Australia and New Zealand. *Cladistics* **23**, 337–361. doi:10.1111/j.1096-0031.2007.00149.x

Clouse, R. M., and Giribet, G. (2007). Across Lydekker's Line – first report of mite harvestmen (Opiliones: Cyphophthalmi: Stylocellidae) from New Guinea. *Invertebrate Systematics* **21**, 207–227. doi:10.1071/IS06046

Clouse, R. M., General, D. M., Diesmos, A. C., and Giribet, G. (2011). An old lineage of Cyphophthalmi (Opiliones) discovered on Mindanao highlights the need for biogeographical research in the Philippines. *The Journal of Arachnology* **39**, 147–153. doi:10.1636/Ha10-108.1

Clouse, R. M., Sharma, P. P., Stuart, J. C., Davis, L. R., Giribet, G., Boyer, S. L., and Wheeler, W. C. (2016). Phylogeography of the harvestman genus *Metasiro* (Arthropoda, Arachnida, Opiliones) reveals a potential solution to the Pangean paradox. *Organisms, Diversity & Evolution* **16**, 167–184. doi:10.1007/s13127-015-0233-7

de Bivort, B. L., and Giribet, G. (2004). A new genus of cyphophthalmid from the Iberian Peninsula with a phylogenetic analysis of the Sironidae (Arachnida: Opiliones: Cyphophthalmi) and a SEM database of external morphology. *Invertebrate Systematics* **18**, 7–52. doi:10.1071/IS03029

Derkarabetian, S., Castillo, S., Koo, P. K., Ovchinnikov, S., and Hedin, M. (2019). A demonstration of unsupervised machine learning in species delimitation. *Molecular Phylogenetics and Evolution* **139**, 106562. doi:10.1016/j.ympev.2019.106562

Fernández, R., and Giribet, G. (2014). Phylogeography and species delimitation in the New Zealand endemic, genetically hypervariable harvestman species, *Aoraki denticulata* (Arachnida, Opiliones, Cyphophthalmi). *Invertebrate Systematics* **28**, 401–414. doi:10.1071/IS14009

Fontaine, B., Perrard, A., and Bouchet, P. (2012). 21 years of shelf life between discovery and description of new species. *Current Biology* **22**, R943–R944. doi:10.1016/j.cub.2012.10.029

Giribet, G. (2003). *Karripurcellia*, a new pettalid genus (Arachnida: Opiliones: Cyphophthalmi) from Western Australia, with a cladistic analysis of the family Pettalidae. *Invertebrate Systematics* **17**, 387–406. doi:10.1071/IS02014

Giribet, G. (2007). Efficient tree searches with available algorithms. *Evolutionary Bioinformatics Online* **3**, 341–356. doi:10.1177/117693430700300014

Giribet, G. (2011). *Shearogovea*, a new genus of Cyphophthalmi (Arachnida, Opiliones) of uncertain position from Oaxacan caves, Mexico. *Breviora* **528**, 1–7. doi:10.3099/528.1

Giribet, G., and Baker, C. M. (2019). Further discussion on the Eocene drowning of New Caledonia: discordances from the point of view of zoology. *Journal of Biogeography* **46**, 1912–1918. doi:10.1111/jbi.13635

Giribet, G., and Boyer, S. L. (2002). A cladistic analysis of the cyphophthalmid genera (Opiliones, Cyphophthalmi). *The Journal of Arachnology* **30**, 110–128. doi:10.1636/0161-8202(2002)030[0110:ACAOTC]2.0.CO;2

Giribet, G., Sharma, P. P., and Bastawade, D. B. (2007). A new genus and species of Cyphophthalmi (Arachnida: Opiliones) from the north-eastern states of India. *Zoological Journal of the Linnean Society* **151**, 663–670. doi:10.1111/j.1096-3642.2007.00347.x

Giribet, G., Sharma, P. P., Benavides, L. R., Boyer, S. L., Clouse, R. M., de Bivort, B. L., Dimitrov, D., Kawauchi, G. Y., Murienne, J. Y., and Schwendinger, P. J. (2012). Evolutionary and biogeographical history of an ancient and global group of arachnids (Arachnida: Opiliones: Cyphophthalmi) with a new taxonomic arrangement. *Biological Journal of the Linnean Society. Linnean Society of London* **105**, 92–130. doi:10.1111/j.1095-8312.2011.01774.x

Giribet, G., McIntyre, E., Christian, E., Espinasa, L., Ferreira, R. L., Francke, Ó. F., Harvey, M. S., Isaia, M., Kováč, L., McCutchen, L., Souza, M. F. V. R., and Zagmajster, M. (2014). The first phylogenetic analysis of Palpigradi (Arachnida) – the most enigmatic arthropod order. *Invertebrate Systematics* **28**, 350–360. doi:10.1071/IS13057

Giribet, G., Buckman-Young, R. S., Sampaio Costa, C., Baker, C. M., Benavides, L. R., Branstetter, M. G., Daniels, S. R., and Pinto-da-Rocha, R. (2018). The '*Peripatos*' in Eurogondwana? – Lack of evidence that south-east Asian onychophorans walked through Europe. *Invertebrate Systematics* **32**, 842–865. doi:10.1071/IS18007

Goloboff, P. A. (1999). Analyzing large data sets in reasonable times: solutions for composite optima. *Cladistics* **15**, 415–428. doi:10.1111/j.1096-0031.1999.tb00278.x

Goloboff, P. A. (2002). Techniques for analyzing large data sets. In 'Techniques in Molecular Systematics and Evolution'. (Eds R. DeSalle, G. Giribet, and W. Wheeler.) pp. 70–79. (Brikhäuser Verlag: Basel.)

Harvey, M. S. (2002). Short-range endemism among the Australian fauna: some examples from non-marine environments. *Invertebrate Systematics* **16**, 555–570. doi:10.1071/IS02009

Harvey, M. S., Rix, M. G., Framenau, V. W., Hamilton, Z. R., Johnson, M. S., Teale, R. J., Humphreys, G., and Humphreys, W. F. (2011). Protecting the innocent: studying short-range endemic taxa enhances conservation outcomes. *Invertebrate Systematics* **25**, 1–10. doi:10.1071/IS11011

Harvey, M. S., Rix, M. G., Harms, D., Giribet, G., Vink, C. J., and Walter, D. E. (2017). The biogeography of Australasian arachnids. In 'Handbook of Australasian Biogeography'. (Ed. M. C. Ebach.) pp. 241–267. (CRC/Taylor and Francis Group.)

Juberthie, C. (1970). Les genres d'opilions Sironinae (Cyphophthalmes). *Bulletin du Muséum National d'Histoire Naturelle, 2e série* **41**, 1371–1390.

Juberthie, C. (1979). Un Cyphophthalme nouveau d'une grotte de Nouvelle-Calédonie: *Troglosiro aelleni* n. gen., n. sp. (Opilion Sironinae). *Revue Suisse de Zoologie* **86**, 221–231. doi:10.5962/bhl.part.82287

Kalyaanamoorthy, S., Minh, B. Q., Wong, T. K. F., von Haeseler, A., and Jermiin, L. S. (2017). ModelFinder: fast model selection for accurate phylogenetic estimates. *Nature Methods* **14**, 587–589. doi:10.1038/nmeth.4285

Kapli, P., Lutteropp, S., Zhang, J., Kobert, K., Pavlidis, P., Stamatakis, A., and Flouri, T. (2017). Multi-rate Poisson tree processes for single-locus species delimitation under maximum likelihood and Markov chain Monte Carlo. *Bioinformatics* **33**, 1630–1638. doi:10.1093/bioinformatics/btx025

Katoh, K., Rozewicki, J., and Yamada, K. D. (2019). MAFFT online service: multiple sequence alignment, interactive sequence choice and visualization. *Briefings in Bioinformatics* **20**, 1160–1166. doi:10.1093/bib/bbx108

Kimura, M. (1980). A simple method for estimating evolutionary rates of base substitutions through comparative studies of nucleotide sequences. *Journal of Molecular Evolution* **16**, 111–120. doi:10.1007/BF01731581

Kuraku, S., Zmasek, C. M., Nishimura, O., and Katoh, K. (2013). aLeaves facilitates on-demand exploration of metazoan gene family trees on MAFFT sequence alignment server with enhanced interactivity. *Nucleic Acids Research* **41**, W22–W28. doi:10.1093/nar/gkt389

Murphree, C. S. (1988). Morphology of the dorsal integument of ten opilionid species (Arachnida, Opiliones). *The Journal of Arachnology* **16**, 237–252.

Myers, N., Mittermeier, R. A., Mittermeier, C. G., da Fonseca, G. A., and Kent, J. (2000). Biodiversity hotspots for conservation priorities. *Nature* **403**, 853–858. doi:10.1038/35002501

Nattier, R., Pellens, R., Robillard, T., Jourdan, H., Legendre, F., Caesar, M., Nel, A., and Grandcolas, P. (2017). Updating the phylogenetic

dating of New Caledonian biodiversity with a meta-analysis of the available evidence. *Scientific Reports* **7**, 3705. doi:10.1038/s41598-017-02964-x

Nguyen, L.-T., Schmidt, H. A., von Haeseler, A., and Minh, B. Q. (2015). IQ-TREE: a fast and effective stochastic algorithm for estimating maximum-likelihood phylogenies. *Molecular Biology and Evolution* **32**, 268–274. doi:10.1093/molbev/msu300

Nixon, K. C. (1999). The Parsimony Ratchet, a new method for rapid parsimony analysis. *Cladistics* **15**, 407–414. doi:10.1111/j.1096-0031.1999.tb00277.x

Oberski, J. T., Sharma, P. P., Jay, K. R., Coblens, M. J., Lemon, K. A., Johnson, J. E., and Boyer, S. L. (2018). A dated molecular phylogeny of mite harvestmen (Arachnida: Opiliones: Cyphophthalmi) elucidates ancient diversification dynamics in the Australian Wet Tropics. *Molecular Phylogenetics and Evolution* **127**, 813–822. doi:10.1016/j.ympev.2018.06.029

Puillandre, N., Lambert, A., Brouillet, S., and Achaz, G. (2012). ABGD, Automatic Barcode Gap Discovery for primary species delimitation. *Molecular Ecology* **21**, 1864–1877. doi:10.1111/j.1365-294X.2011.05239.x

Schmidt, S. M., Buenavente, P. A. C., Blatchley, D. D., Diesmos, A. C., Diesmos, M. L., General, D. E. M., Mohagan, A. B., Mohagan, D. J., Clouse, R. M., and Sharma, P. P. (2019). A new species of Tithaeidae (Arachnida: Opiliones: Laniatores) from Mindanao reveals contemporaneous colonisation of the Philippines by Sunda Shelf opiliofauna. *Invertebrate Systematics* **33**, 237–251. doi:10.1071/IS18057

Schwentner, M., and Giribet, G. (2018). Phylogeography, species delimitation and population structure of a Western Australian short-range endemic mite harvestman (Arachnida: Opiliones: Pettalidae: *Karripurcellia*). *Evolutionary Systematics* **2**, 81–87. doi:10.3897/evolsyst.2.25274

Sharma, P. P. (2006). On the biogeography of New Caledonia: a revision of the Cyphophthalmi of New Caledonia with a phylogenetic analysis of the Troglosironidae (Arachnida, Opiliones, Cyphophthalmi). Undergraduate Senior Thesis, Harvard University.

Sharma, P., and Giribet, G. (2005). A new *Troglosiro* species (Opiliones, Cyphophthalmi, Troglosironidae) from New Caledonia. *Zootaxa* **1053**, 47–60. doi:10.11646/zootaxa.1053.1.4

Sharma, P., and Giribet, G. (2009*a*). A relict in New Caledonia: phylogenetic relationships of the family Troglosironidae (Opiliones: Cyphophthalmi). *Cladistics* **25**, 279–294. doi:10.1111/j.1096-0031.2009.00252.x

Sharma, P. P., and Giribet, G. (2009*b*). The family Troglosironidae (Opiliones: Cyphophthalmi) of New Caledonia. In 'Zoologia Neocaledonica. 7. Biodiversity Studies in New Caledonia'. (Ed. P. Grandcolas.) pp. 83–123 (Mémoires du Muséum national d'Histoire naturelle: Paris, France.)

Sharma, P. P., Vahtera, V., Kawauchi, G. Y., and Giribet, G. (2011). Running $_{W}$ILD: The case for exploring mixed parameter sets in sensitivity analysis. *Cladistics* **27**, 538–549. doi:10.1111/j.1096-0031.2010.00345.x

Shear, W. A. (1993). The genus *Troglosiro* and the new family Troglosironidae (Opiliones, Cyphophthalmi). *The Journal of Arachnology* **21**, 81–90.

Sutherland, R., Dickens, G. R., Blum, P., Agnini, C., Alegret, L., Asatryan, G., Bhattacharya, J., Bordenave, A., Chang, L., Collot, J., Cramwinckel, M. J., Dallanave, E., Drake, M. K., Etienne, S. J. G., Giorgioni, M., Gurnis, M., Harper, D. T., Huang, H.-H. M., Keller, A. L., Lam, A. R., Li, H., Matsui, H., Morgans, H. E. G., Newsam, C., Park, Y.-H., Pascher, K. M., Pekar, S. F., Penman, D. E., Saito, S., Stratford, W. R., Westerhold, T., and Zhou, X. (2020). Continental-scale geographic change across Zealandia during Paleogene subduction initiation. *Geology* **48**, 419–424. doi:10.1130/G47008.1

Trifinopoulos, J., Nguyen, L.-T., von Haeseler, A., and Minh, B. Q. (2016). W-IQ-TREE: a fast online phylogenetic tool for maximum likelihood analysis. *Nucleic Acids Research* **44**, W232–W235. doi:10.1093/nar/gkw256

Wheeler, W. C. (1995). Sequence alignment, parameter sensitivity, and the phylogenetic analysis of molecular data. *Systematic Biology* **44**, 321–331. doi:10.2307/2413595

Wheeler, W. (1996). Optimization alignment: the end of multiple sequence alignment in phylogenetics? *Cladistics* **12**, 1–9. doi:10.1111/j.1096-0031.1996.tb00189.x

Wheeler, W. C. (2003). Implied alignment: a synapomorphy-based multiple-sequence alignment method and its use in cladogram search. *Cladistics* **19**, 261–268. doi:10.1111/j.1096-0031.2003.tb00369.x

Wheeler, W. C., Aagesen, L., Arango, C. P., Faivovich, J., Grant, T., D'Haese, C., Janies, D., Smith, W. L., Varón, A., and Giribet, G. (2005). 'Dynamic Homology and Phylogenetic Systematics: a Unified Approach using POY.' (American Museum of Natural History: New York.)

Wheeler, W. C., Lucaroni, N., Hong, L., Crowley, L. M., and Varón, A. (2015). POY version 5: phylogenetic analysis using dynamic homologies under multiple optimality criteria. *Cladistics* **31**, 189–196. doi:10.1111/cla.12083

Willemart, R. H., and Giribet, G. (2010). A scanning electron microscopic survey of the cuticle in Cyphophthalmi (Arachnida, Opiliones) with the description of novel sensory and glandular structures. *Zoomorphology* **129**, 175–183. doi:10.1007/s00435-010-0110-z

Zhang, J., Kapli, P., Pavlidis, P., and Stamatakis, A. (2013). A general species delimitation method with applications to phylogenetic placements. *Bioinformatics* **29**, 2869–2876. doi:10.1093/bioinformatics/btt499

Handling editor: Mark Harvey